THE JOURNAL OF PHYSICAL CHEMISTRY A



Article

# High-Resolution Near Infrared Spectroscopy and Vibrational Dynamics of Dideuteromethane (CHD)

O. N. Ulenikov, E. S. Bekhtereva, S. Albert, S. Bauerecker, H. Hollenstein, and M. Quack

*J. Phys. Chem. A*, **2009**, 113 (10), 2218-2231• DOI: 10.1021/jp809839t • Publication Date (Web): 05 March 2009

# High-Resolution Near Infrared Spectroscopy and Vibrational Dynamics of Dideuteromethane ($CH_2D_2$)†

**O. N. Ulenikov,[‡,§] E. S. Bekhtereva,[‡,§] S. Albert,[‡] S. Bauerecker,[‡,||] H. Hollenstein,[‡] and M. Quack*[,‡]**

*Physical Chemistry, ETH Zürich, CH-8093 Zürich, Switzerland, Laboratory of Molecular Spectroscopy, Physics Department, Tomsk State University, Tomsk, 634050, Russia, and Technische Universität Braunschweig, D - 38106, Braunschweig, Germany*

*Received: November 7, 2008; Revised Manuscript Received: December 22, 2008*

We report the infrared spectrum of $CH_2D_2$ measured in the range from 2800 to 6600 $cm^{-1}$ with the Zürich high-resolution Fourier transform interferometer Bruker IFS 125 prototype (ZP 2001, with instrumental bandwidth less than $10^{-3}$ $cm^{-1}$) at 78 K in a collisional enclosive flow cooling cell used in the static mode. Precise experimental values (with uncertainties between 0.0001 and 0.001 $cm^{-1}$) were obtained for the band centers by specific assignment of transitions to the $J = 0$ level of 71 vibrational levels. In combination with 22 previously known band centers, these new results were used as the initial information for the determination of the harmonic frequencies, force constant parameters $F_{ij}$, anharmonic coefficients, and vibrational resonance interaction parameters. A set of 47 fitted parameters for an effective Hamiltonian reproduces the vibrational level structure of the $CH_2D_2$ molecule up to 6600 $cm^{-1}$ with a root-mean-square deviation $d_{rms} = 0.67$ $cm^{-1}$. The results are discussed in relation to the multidimensional potential hypersurface of methane and its vibrational dynamics.

## 1. Introduction

The vibrational spectroscopy and vibrational dynamics of polyatomic molecules on multidimensional Born−Oppenheimer potential hypersurfaces has been a long standing problem of molecular spectroscopy and molecular physics.[1−3] The traditional approach to relate spectra and properties of potential hypersurfaces has been to start out from the harmonic approximation and to derive anharmonic potential constants in a Taylor series expansion by means of fitting effective Hamiltonians derived from perturbation theory to experimental rovibrational spectra.[4−12] However, it was recognized some time ago that for an accurate description of the relation between spectra, vibrational dynamics, and potential hypersurfaces vibrational (and rovibrational) variational calculations are necessary. Max Wolfsberg and his colleagues have been among the pioneers in this field with early calculations on $H_2O$ and $CH_2O$[13−16] about a quarter century ago. Over the years numerous calculations of increasing accuracy have been reported for these two semirigid molecules, and we quote here as examples (from a very large literature on the topic) only a few (see ref 17−22 and references cited therein). Also the question of spectra and dynamics of nonrigid molecules and clusters has been tackled successfully by formulating global potential hypersurfaces and carrying out full dimensional variational quantum dynamical calculations including tunneling processes for up to four-atom systems such as the dimer $(HF)_2$ of hydrogen fluoride[23−26] and also the hydrogen peroxide molecule (HOOH) with the possibility of picosecond stereomutation tunneling.[27−29]

Another important example in the development of our understanding of relating spectra, dynamics, and potential hypersurfaces is the organic prototype molecule methane. Here, it was recognized in the 1980s that, for instance, the effective Hamiltonian anharmonic Fermi resonance coupling constant $k_{sbb}$ (30 $cm^{-1}$) differed from the corresponding potential constant $C_{sbb}$ (150 $cm^{-1}$) by about a factor of 5, when properly relating potentials and spectra with vibrational variational calculations on accurate potential hypersurfaces (MRD-CI and beyond),[30−34] although from simple perturbation theory they would be equal. While the early variational calculations for methane were still of reduced dimensionality, today fully 9-dimensional vibrational variational calculations on global potential hypersurfaces for $CH_4$ can be considered to be the frontier of such research.[35−45]

In this context, but also because of the importance of methane in many fields of science ranging from reactions kinetics and combustion science to geology, from environmental and planetary science to astrophysics, we have initiated some time ago a detailed study of rovibrational spectra of the methane isotopomer $CH_2D_2$ with the goal of obtaining an as complete understanding of its vibrational dynamics as possible.[46,47] $CH_2D_2$ (Figure 1) is particularly suited for a study of its rovibrational dynamics, as it is the

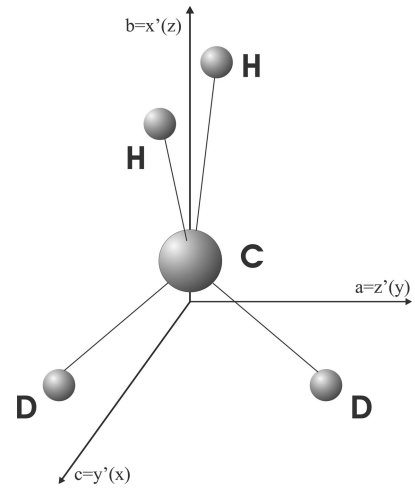


**Figure 1.** Axes definitions used in the present work for dideuteromethane ($CH_2D_2$). The unprimed symbols refer to the axis definitions for the $C_{2v}$ symmetry group used in the classification of the vibrational modes. The primed symbols refer to the Cartesian axis definitions of the $I^r$ representation of Watson's *A*-reduced effective Hamiltonian.

† Part of the "Max Wolfsberg Festschrift".

* Corresponding author. ETH Zürich, Laboratorium für Physikalische Chemie, Wolfgang-Pauli-Strasse 10, CH-8093 Zürich, Switzerland. Phone: +41-44-632 44 22. Fax: +41-44-633 15 98. E-mail: martin@quack.ch.

‡ ETH Zürich.

§ Tomsk State University.

|| Technische Universität Braunschweig.

10.1021/jp809839t CCC: $40.75 
Published on Web 03/05/2009

**TABLE 1: Values of the Fundamental Band Centers of $CH_2D_2$ (in $cm^{-1}$)[a]**

| $\nu$ | $\Gamma^b$ | $\nu_0^{exp}/cm^{-1}$ | ref | assignment[b] |
|---|---|---|---|---|
| $\nu_1$ | $A_1$ | 2975.4823 | [this work] | $CH_2$ s-stretching |
| $\nu_2$ | $A_1$ | 2203.2171 | 46, 47, 60 | $CD_2$ s-stretching |
| $\nu_3$ | $A_1$ | 1435.1346 | 46, 47, 59 | $CH_2$ scissoring |
| $\nu_4$ | $A_1$ | 1033.0534 | 46, 47, 59 | $CD_2$ scissoring |
| $\nu_5$ | $A_2$ | 1331.4087 | 46, 47 | $CH_2$ twisting |
| $\nu_6$ | $B_1$ | 3012.2595 | [this work] | $CH_2$ a-stretching |
| $\nu_7$ | $B_1$ | 1091.185 | 46, 47, 59 | $CH_2$ rocking |
| $\nu_8$ | $B_2$ | 2234.6923 | 46, 47, 60 | $CD_2$ a-stretching |
| $\nu_9$ | $B_2$ | 1236.2771 | 46, 47, 59 | $CH_2$ wagging |

[a] See also ref 47 and references cited therein. [b] s for symmetric, a for antisymmetric, $\Gamma$ gives the species of the mode in the point group $C_{2v}$(see Figure 1).

only nonradioactive asymmetric top isotopomer of methane, where the lowered symmetry places fewer restrictions on the electric dipole transitions and removes complications from degenerate vibrational modes as compared to the more highly symmetric isotopomers of $C_{3v}$ and $T_d$ symmetry.

There exists, of course, a substantial body of spectroscopic work on $CH_2D_2$. Table 1 summarizes the nine vibrational fundamentals as known today. A total of 22 vibrational bands had been studied at moderate to high resolution prior to the present work, where we reanalyze also three of the previously known bands.[48−60] The far-infrared pure rotational spectrum has also been studied with the main goal of deriving the permanent dipole moment of $CH_2D_2$ including the answer to the long standing question of its sign.[61,62]

In our two previous papers, we have complemented the low-energy spectra by observing and analyzing previously undetected, weak, or forbidden transitions for example to levels of $A_2$ symmetry or weaker overtone and combinations levels.[46,47] The goal of the present investigation is to very substantially increase our knowledge of the vibrational spectra and dynamics of $CH_2D_2$ to energies extending beyond $E/hc = 6000\ cm^{-1}$. To achieve such a goal, one may distinguish two strategies. The first one would be to systematically study with stepwise increasing energy all the interacting rovibrational polyads or band systems by means of a complete rovibrational analysis of all observable rovibrational transitions up to a given energy. This is an enormous task, which for the parent isotopomer $CH_4$ has recently been completed just to the octad[63] (i.e., all levels up to about 4600 $cm^{-1}$) and for $^{13}CH_4$ up to the pentad[64] (i.e., 3100 $cm^{-1}$), the octad analysis still being in progress but near to completion. Such complete analyses by necessity can progress only slowly to higher levels of excitation.

A second strategy consists of using spectra taken at low temperatures, which allow for a partial analysis and assignment of spectral lines just for low angular momentum quantum numbers and in particular an assignment and precise measurement of spectral lines belonging to transitions to the $J = 0$ rotational level of the excited vibrational state considered. In this way, one obtains a precise experimental result for the pure vibrational energy for the state considered. For example, this strategy using supersonic jet cavity ring down spectroscopy has been successful in precisely locating the $(\nu_2 + 2\nu_3)$ level of the icosad of $CH_4$ at 7510.3378 $cm^{-1}$, far beyond the range accessible to analysis by the first strategy.[65,66] One might also note that even the complete rovibrational analyses of the first strategy, when using room temperature spectra, sometimes cannot directly assign the $J = 0$ levels, if only lines corresponding to higher rotational quantum numbers are accessible by such spectra. Thus the vibrational band centers derived from such analyses frequently do not include a direct observation of the pure vibrational energy, even though an accurate and complete analysis in general can be relied on in providing also the pure vibrational energy correctly.

We shall discuss and illustrate the power of the present second strategy in assigning vibrational levels directly in the following sections. Indeed, we have been able to accurately locate about 70 additional vibrational level positions beyond the ones (22) previously known from many years of research. Figure 2 gives an overview of the number of assigned vibrational levels compared to the total number of expected levels. We shall discuss also the implications of these new results for our understanding of the vibrational dynamics and potential hypersurfaces of methane in the last section of our paper.

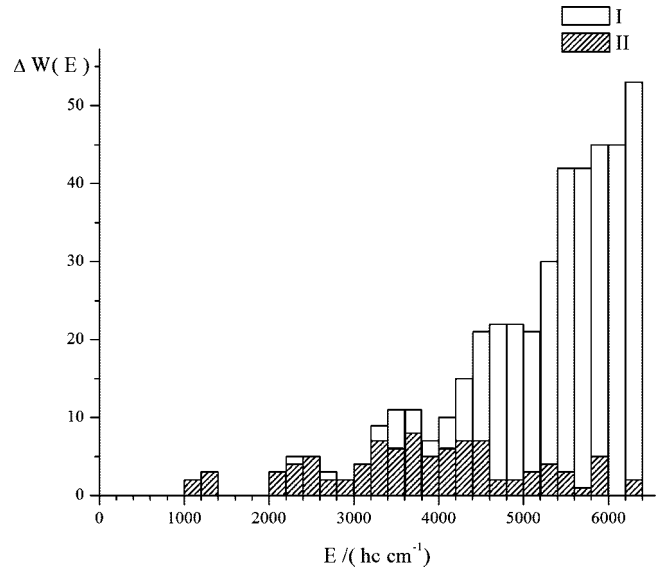


**Figure 2.** Diagram of the "density" of "cold" (0 K) vibrational bands of the $CH_2D_2$ molecule in the region below 6500 $cm^{-1}$ (equivalent to the density of levels, i.e., including "forbidden" bands). The diagram shows the number $\Delta W(E_i)$ of levels in intervals $i$ of 200 $cm^{-1}$ for each interval from 0 to 6400 $cm^{-1}$. The sum $\sum_{i=0}^{N(E)} \Delta W(E_i)$ is the total number of levels $W(E)$ below $E$. I - total number of possible bands (calculated from the data in Table 6). II - number of bands assigned up to now from experimental spectra (see Table 5).

## 2. Experimental

The Fourier transform infrared (FTIR) spectrum of $CH_2D_2$ has been recorded in the wavenumber range from 2800 to 6600 $cm^{-1}$ with the Zürich FTIR spectrometer Bruker IFS 125 prototype 2001.[67,68] The nominal instrumental resolution, defined by 1/MOPD (maximum optical path difference) ranged from 0.0027 to 0.0048 $cm^{-1}$ resulting in essentially Doppler limited spectra. The Doppler widths at 78 K range from about 0.004 $cm^{-1}$ at 2800 $cm^{-1}$ to 0.0096 $cm^{-1}$ at 6600 $cm^{-1}$. About 100 spectra were typically coadded in each spectral region. A newly built enclosive flow cooling cell based on White optics and embedded in a Dewar was used for recording the cold spectra[69] similar to the design described in refs 70−72. The cooling cell was connected via an evacuated transfer optics chamber to the external parallel port of our spectrometer.[69] It was used here in the static mode (without permanent flow). Optical path lengths ranging from 5 to 10 m were used for the measurements. More details of the experimental setup and procedures can be found in ref 69. A preliminary report of the present work has already been provided in ref 73.

Most of the $CH_2D_2$ spectra were taken at 78 K. The total sample pressure of a mixture of $CH_2D_2$ and He in the cell ranged from 2.8 to 3.5 mbar in most cases. In addition, spectra with a pressure of 0.5 mbar were recorded to measure the strong lines without saturation. Pressure broadening can be neglected under these conditions. All spectra were self-apodized. The aperture used was 1 mm. Table 2 summarizes the experimental parameters. The spectra were calibrated with OCS at room temperature (2900 to 3600 $cm^{-1}$)[74] and with $^{12}CH_4$ from 3000 to 6000 $cm^{-1}$.[75] The $CH_2D_2$ sample was purchased from Cambridge

**TABLE 2: Experimental Setup for the Regions 2800−6600 cm$^{-1}$ of the Infrared Spectrum of $CH_2D_2$**

| region/ cm$^{-1}$ | resolution/ cm$^{-1}$ | windows | source | detector | beamsplitter | opt. filter/ cm$^{-1}$ | aperture/ mm | $\nu_{mirror}$/ (kHz) | electr. filter/ cm$^{-1}$ | calib. gas |
|---|---|---|---|---|---|---|---|---|---|---|
| 2800−3700 | 0.0027 | KBr | Globar | InSb | $CaF_2$ | 3000−3600 | 1.0 | 40 | 2370−3950 | OCS[74] |
| 3200−4600 | 0.0033 | KBr | Tungsten | InSb | $CaF_2$ | 3350−4450 | 1.0 | 40 | 2765−5529 | $CH_4$[75] |
| 4200−5600 | 0.0040 | KBr | Tungsten | InSb | $CaF_2$ | 4350−5500 | 1.0 | 40 | 2765−7109 | $CH_4$[75] |
| 5200−6400 | 0.0047 | KBr | Tungsten | InSb | $CaF_2$ | 5350−6350 | 1.0 | 42 | 3950−7109 | $CH_4$[75] |

Isotope Laboratories. The identity, chemical, and isotopic purity (specified to be better than 98%) were obvious from the spectra.

The relative wavenumber accuracy of nonblended, unsaturated, and not too weak lines (about 8500 assignments) can be estimated to be better than $10^{-6}$ cm$^{-1}$ in the range from 2800 to 6600 cm$^{-1}$. The absolute wavenumber accuracy depends upon the accuracy of the reference lines used for calibration, which have an uncertainty of about $10^{-4}$ cm$^{-1}$ for the lower wavenumber range and between $10^{-4}$ and $10^{-3}$ cm$^{-1}$ for the higher wavenumber range extending beyond 6000 cm$^{-1}$.

## 3. Analysis of the Experimental Spectrum

Figure 3 shows an overview of the experimental FTIR spectrum. As shown above in Figure 2, the density of possible vibrational bands is rapidly increasing with increasing energy. The spectrum is characterized by some strong bands corresponding to first overtone and simple binary combination bands (the total number of this kind of bands allowed in absorption is 37) and further much weaker second overtone and more complex combination bands corresponding to triple excitations (the total number of such infrared bands is 127). The bands which correspond to excitations with four and more vibrational quanta are extremely weak and were not visible in the spectra, as a rule. However, because of some strong resonance interactions even weak third overtone and more complex combination bands can sometimes be identified in the experimental spectrum. In any case, the experimental conditions described in Section 2 allowed us to newly assign 71 vibrational bands which one can compare with the smaller number, 22, of bands studied with high resolution in all previous work together. Transitions with quantum number $J \leq 8$ to 12 for the strong bands and $J \leq 5$ to 6 for the weak bands were assigned in the spectra recorded at a temperature of 78 K.

Figure 4 illustrates the great simplification and improvement of the spectral data obtained in the cold cell at 78 K (upper part) compared to the room temperature spectrum (lower part) in the small spectral range shown around 4441 cm$^{-1}$. At room temperature, one finds many overlapping, blended, and also weak lines. By contrast, in the cold cell spectrum, the lines are well separated and sharp because of the smaller Doppler widths, often with excellent signal-to-noise ratio, about 500:1 for strong lines and 3:1 for the weakest lines. As discussed in the Introduction, the cold cell spectra allowed us to considerably simplify the assignment of spectra and the identification of pure vibrational level energies. This is illustrated by the level scheme in Figure 5, which shows the ground-state level, the excited rotational levels of the vibrational ground-state with $J'' = 1$, and the possible combinations of $K''_a$ and $K''_c$. These rotational levels form the possible lower levels for selectively assigned transitions connecting to a rotationless upper vibrational level.

In the case when the upper vibrational state is of $A_1$-symmetry, one has $K''_a = K''_c = 1$. Analogously, $K''_a = 0$, $K''_c = 1$ applies when the upper vibrational state has the symmetry $B_2$ or $K''_a = 1$, $K''_c = 0$ for $B_1$ upper level symmetry. The transition to an upper vibrational level of $A_2$ symmetry species is forbidden, and such levels have to be measured by other means.[46,47] It should be mentioned that while all the other upper rovibrational levels of a vibrational level are reached by more than one transition, and thus the identities can be confirmed by the corresponding combination differences, the $E_{[J'=0, K'_a=0, K'_c=0]}$ upper rovibrational level (and as a consequence, the "experimental" value of the band center, as well) can be obtained from only one transition as indicated in Figure 5. Therefore, the problem of a correct search for this selected transition in the experimental spectrum is important. This was done in the following way: Fits of the sets of energies of the type $E_{[J', K'_a=0, K'_c=J']}$ ($J' = 1, 2, 3, 4,...$) have been carried out for all bands studied. This allowed us to predict the position of the $[J' = 0,\ K'_a = 0,\ K'_c = 0](\upsilon') \leftarrow [J'' = 1,\ K''_a,\ K''_c]$ ($\upsilon''$) transition with an accuracy of about 0.01−0.06 cm$^{-1}$. This accuracy is sufficient to identify beyond doubt the corresponding line in our experimental spectrum.

To illustrate this procedure, Table 3 presents the predicted line positions for the transitions $[J' = 0,\ K'_a = 0,\ K'_c = 0](\upsilon') \leftarrow [J'' = 1,\ K''_a, K''_c](\upsilon'' = 0)$, in comparison with the experimental line positions for 10 of the lower wavenumber bands analyzed. The matching leaves no room for ambiguity. As an additional confirmation of the correctness of this assignment procedure, the "smooth" behavior of the line strengths in the sets of transitions $[J', K'_a = 0, K'_c = J'](\upsilon') \leftarrow [J'' = J' + 1, K''_a = 0/1, K''_c = J' + 1/J'](\upsilon'' = 0)$ can be mentioned. Figure 6a, 6b, and 6c give an illustration of the procedure for three bands of different symmetry. One can see very nicely the various assigned transitions of the bands and the convergence to the predicted selected lines marked by the arrows. These lines provide thus the transitions to the rotationless upper vibrational levels, and by adding the rotational energies of the lower level of the transition one obtains as indicated in Table 3 finally the upper vibrational energy $E'_{vib}$.

The lower level rotational energies in Figure 5 cannot be obtained from the pure rotational transitions or from simple combination differences, as the corresponding transitions are forbidden by symmetry in $C_{2v}$. However, we have reanalyzed numerous ground-state combination differences in terms of rotational energies for low $J$ levels and derived the relevant $J = 1$ level energies in Figure 5 from the appropriate fit of effective rotational Hamiltonian constants to the spectral data. This extrapolation to $J = 1$ level energies provides the data for $E''_{rot}$ in Table 3 with an accuracy of at least five significant digits. Therefore, the remaining uncertainty does not affect the upper vibrational level energies determined by adding the transition energy to the lower level rotational energy. Table 4 gives the corresponding rotational parameters.

In total, more than 8500 rovibrational transitions were assigned to 71 excited vibrational levels. More than 8400 of these transitions were confirmed by combination differences. The list of experimental band centers is given in Table 5 together with all calculated levels as described in Section 4 in detail. When four digits after the decimal point are given for the experimental result, then the band center was derived directly by the procedure described above. These data should have an uncertainty limited only by the calibration and peak finding uncertainties, which are in the range between 0.0001 and 0.001 cm$^{-1}$ (see Section 2). The complete listing of all assigned rovibrational transitions will be reported in conjunction with a partially complete rovibrational analysis including interactions for high $J$ levels.[76]

In a few cases, we were able to estimate the band center only by a less accurate fit procedure. For these four levels, we give only one digit after the decimal point, and we did not use those data in

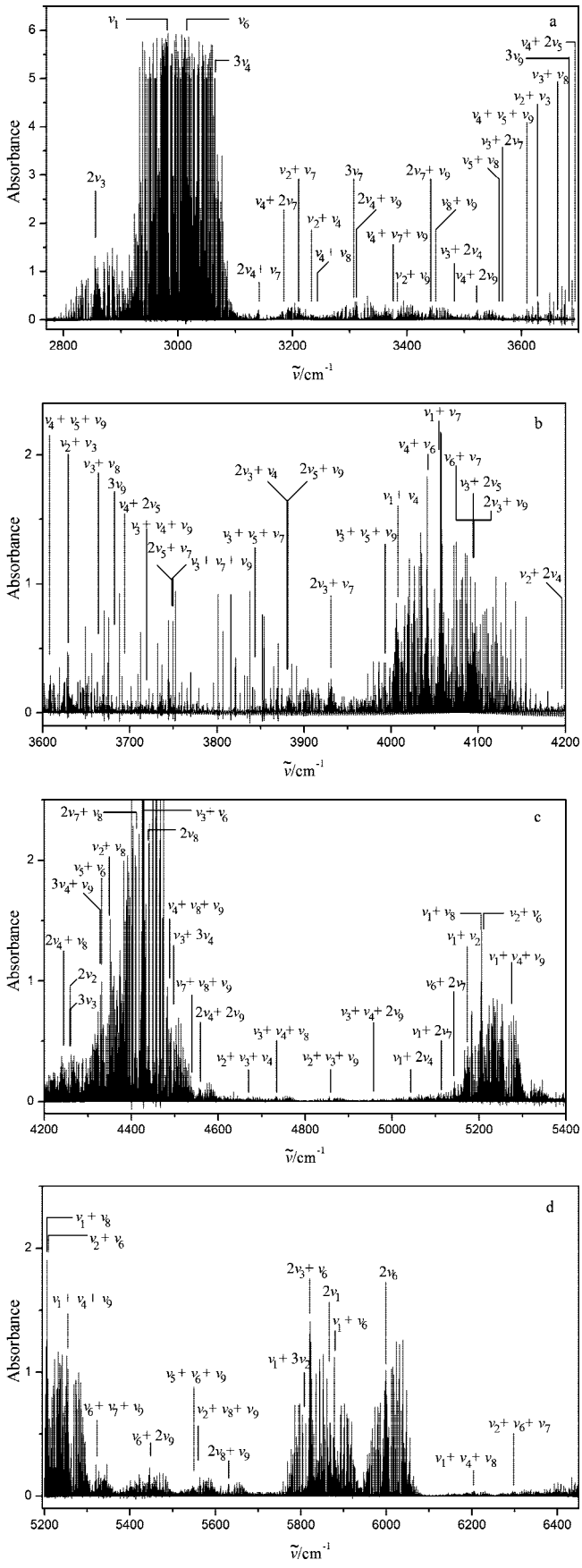


**Figure 3.** Survey spectrum of $CH_2D_2$ in the region of 2800−6500 cm$^{-1}$. Experimental conditions are presented in Table 1. The parts a, b, c, d cover the range from 2800 to 6400 cm$^{-1}$. The decadic absorbance lg($I_0$/$I$) is given on the ordinate.

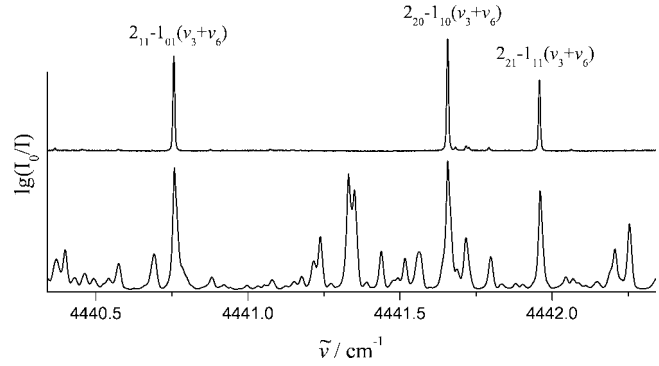


**Figure 4.** Small portion of the spectrum of the $CH_2D_2$ molecule in the region of the $\nu_3 + \nu_6$ band. Upper trace: Bruker IFS 125 prototype (ZP 2001) spectrum at 78 K. Lower trace: Bomem DA002 spectrum at 293 K. Both spectra are essentially Doppler limited.

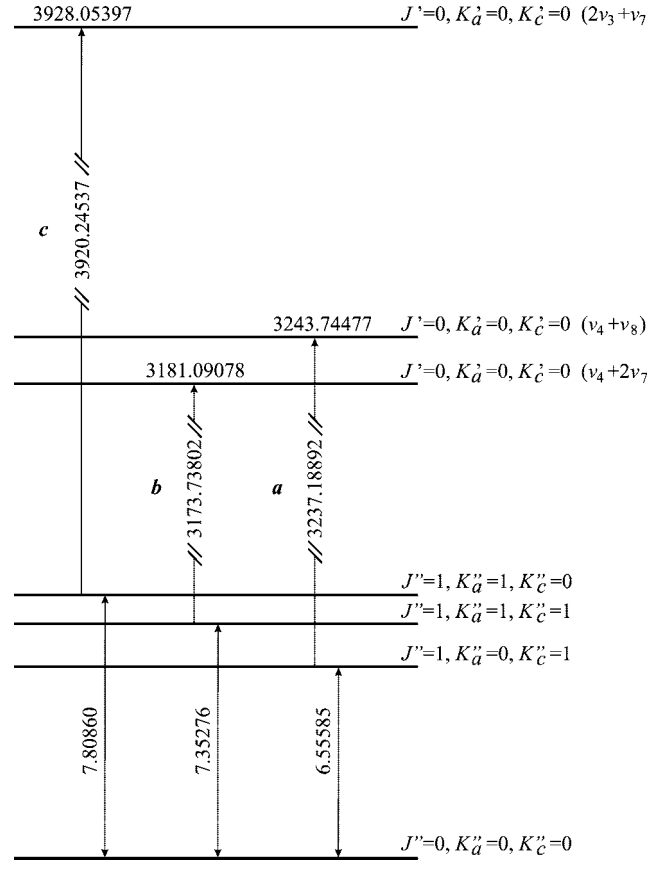


**Figure 5.** Level scheme explaining the procedure to derive the ($J'$ = 0, $v'$) level energy for an excited level $v'$ from experimental transition wavenumbers and ground-state rotational energies. All transition wavenumbers and term values are given in cm$^{-1}$. *a* stands for *a*-type transition, *b* for *b*-type, *c* for *c*-type.

the final fits of data as we cannot specify a definitive uncertainty estimate. These four band centers refer to the $\nu_4 + \nu_7 + \nu_9$, $\nu_3 + \nu_7 + \nu_9$, $\nu_5 + \nu_6$, and $\nu_5 + \nu_8$ bands. The first two correspond to transitions where the upper vibrational state is of $A_2$ symmetry, and as a consequence, they are "forbidden" in absorption. They appear in the spectrum only for $J > 0$ because of strong resonance interactions with neighboring states showing allowed infrared transitions. This circumstance leads to the absence of the transition to the [$J' = 0$, $K_a' = 0$, $K_c' = 0$] upper rovibrational state. Thus, the corresponding band centers cannot be derived from the experimental data and can only be obtained from the fit. Furthermore, also in the cases of the $\nu_5 + \nu_6$ and $\nu_5 + \nu_8$ bands, which are allowed, but very weak, the P-type transitions [$J' = 0$, $K_a' =$

**TABLE 3: Line Positions and Levels for the Transitions $[J' = 0, K'_a = 0, K'_c = 0](v') \leftarrow [J'' = 1, K''_a, K''_c](v'' = 0)$ for Some Absorption Bands of $CH_2D_2$ (in $cm^{-1}$)**

| band | $(0 \leftarrow 1)^{predict.}$ | $(0 \leftarrow 1)^{exp.}$ | $J'' K''_a K''_c$ | $E''_{rot.}/hc$ | $E'_{vib.}/hc$ |
|---|---|---|---|---|---|
| $2\nu_3$ ($A_1$) | 2848.315 | 2848.3122 | 1 1 1 | 7.3528 | 2855.6650 |
| $\nu_1$ ($A_1$) | 2968.130 | 2968.1295 | 1 1 1 | 7.3528 | 2975.4823 |
| $\nu_6$ ($B_1$) | 3004.450 | 3004.4509 | 1 1 0 | 7.8086 | 3012.2595 |
| $3\nu_4$ ($A_1$) | 3058.782 | 3058.7813 | 1 1 1 | 7.3528 | 3066.1341 |
| $2\nu_4 + \nu_7$ ($B_1$) | 3133.876 | 3133.8177 | 1 1 0 | 7.8086 | 3141.6263 |
| $\nu_4 + 2\nu_7$ ($A_1$) | 3173.783 | 3173.7380 | 1 1 1 | 7.3528 | 3181.0908 |
| $\nu_2 + \nu_7$ ($B_1$) | 3202.457 | 3202.4589 | 1 1 0 | 7.8086 | 3210.2675 |
| $\nu_2 + \nu_4$ ($A_1$) | 3226.329 | 3226.3281 | 1 1 1 | 7.3528 | 3233.6809 |
| $\nu_4 + \nu_8$ ($B_2$) | 3237.187 | 3237.1889 | 1 0 1 | 6.5559 | 3243.7448 |
| $3\nu_7$ ($B_1$) | 3298.956 | 3298.9560 | 1 1 0 | 7.8086 | 3306.7646 |

$0, K'_c = 0](v') \leftarrow [J'' = 1,\ K''_a,\ K''_c](v'' = 0)$ could not be identified beyond doubt in the spectrum. Therefore, the centers of the $\nu_5 + \nu_6$ and $\nu_5 + \nu_8$ bands were also not derived from an experimental transition but were estimated from the fit.

The level assignment in the first column of Table 5, given in terms of the excitation of the normal modes, has, of course, limited significance when there is extensive state mixing particularly at higher excitations. The symmetry assignment in $C_{2v}$ (see Figure 1) is, however, robust.

One can see from Table 5 that below about 4500 $cm^{-1}$ the large majority of vibrational levels could actually be observed, whereas the fraction of experimentally assigned levels rapidly decreases above 4500 $cm^{-1}$, many bands being too weak for detection under our conditions (see also Figure 2).

The predictions derived in the following section and summarized in Table 5 as well might help to assign further levels in spectra taken under appropriate conditions.

## 4. Theoretical Background, Symmetry, Hamiltonian Model, and Vibrational Assignment

$CH_2D_2$ is an asymmetric top molecule with $C_{2v}$ point group symmetry (see Figure 1). Its nine vibrational modes $q_K$ have the symmetry species as given for the corresponding fundamentals in Table 1. Similarly, the vibrational wave functions ($v_1$, $v_2$, $v_3$, $v_4$, $v_5$, $v_6$, $v_7$, $v_8$, $v_9$), where the symbol $v_i$ denotes the number of quanta in the $i$-th vibrational mode, belong to one of the four symmetry species $A_1$, $A_2$, $B_1$, or $B_2$.The complete permutation inversion group for $CH_2D_2$ is $S^*_{2,2}$ of order 8;[77,78] however, tunneling is not observed due to the high barrier,[79] and the induced representation $\Gamma(MS_4 \sim C_{2v}) \uparrow \Gamma(S^*_{2,2})$ indicates that both positive and negative parities arise for all sublevels in contrast to $CH_4$ and $CH_3D$. More details of symmetry and nuclear spin statistics are discussed in refs 76 and 80.

As shown in Figure 2, one expects a rapid increase of the density of vibrational states with increasing wavenumber. Furthermore, the infrared spectrum is complicated by the presence of numerous and strong resonance interactions between many vibrational states. As a consequence, even a preliminary analysis of the infrared spectra of the $CH_2D_2$ molecule requires consideration of the relevant resonance interactions both of the Fermi and Darling−Dennison as well as of the Coriolis types. In accordance with the general symmetry properties, such Hamiltonians have the following form[4−11,47,59]

$$H^{v.-r.} = \sum_{v,\tilde{v}} |v\rangle\langle\tilde{v}| H_{v\tilde{v}} \tag{1}$$

where the summation extends over all interacting vibrational states. The diagonal operators $H_{vv}$ describe unperturbed rotational structures of the vibrational states involved. The nondiagonal operators $H_{v\tilde{v}}$, ($v \neq \tilde{v}$) describe different kinds of resonance interactions between the states $|v\rangle$ and $|\tilde{v}\rangle$. The diagonal block operators have the same form for all the vibrational states involved (they are so-called Watson Hamiltonians, here in the A-reduction and $I^r$ representation[81,82])

$$H_{vv} = E^v + \left[A^v - \frac{1}{2}(B^v + C^v)\right]J_z^2 + \frac{1}{2}(B^v + C^v)J^2 + \frac{1}{2}(B^v - C^v)J_{xy}^2 - \Delta_K^v J_z^4 - \Delta_{JK}^v J_z^2 J^2 - \Delta_J^v J^4 - \delta_K^v [J_z^2, J_{xy}^2] - 2\delta_J^v J^2 J_{xy}^2 + \ldots \tag{2}$$

where $J_\alpha$ ($\alpha = x, y, z$) are the components of the angular momentum operator defined in the molecule-fixed coordinate system; $J_{xy}^2 = J_x^2 - J_y^2$; $A^v$, $B^v$, and $C^v$ are the effective rotational constants connected with the vibrational states $v$; and the other parameters are the different centrifugal distortion coefficients.

We can distinguish between four types of coupling operators $H_{v\tilde{v}}$ ($v \neq \tilde{v}$) corresponding to the four different types of resonance interactions which can occur in $C_{2v}$ asymmetric top molecules. If the product $\Gamma = \Gamma^v \otimes \Gamma^{\tilde{v}}$ of the symmetry species of the states $v$ and $\tilde{v}$ is equal to $A_1$ (i.e., $\Gamma^v = \Gamma^{\tilde{v}}$), then the states $v$ and $\tilde{v}$ are connected by an anharmonic resonance interaction, and the corresponding interaction operator has the form

$$H_{v\tilde{v}} = {}^{v\tilde{v}}F_0 + {}^{v\tilde{v}}F_K J_z^2 + {}^{v\tilde{v}}F_J J^2 + \ldots + {}^{v\tilde{v}}F_{xy}(J_x^2 - J_y^2) + \ldots \tag{3}$$

If the product is $\Gamma = B_1$, then the states $v$ and $\tilde{v}$ are connected by a Coriolis resonance interaction of the form

$$H_{v\tilde{v}} = iJ_z H_{v\tilde{v}}^{(1)} + \{J_x, J_y\}_+ H_{v\tilde{v}}^{(2)} + H_{v\tilde{v}}^{(2)}\{J_x, J_y\}_+ + \ldots \tag{4}$$

When $\Gamma = B_2$, the following Coriolis interaction is allowed

$$H_{v\tilde{v}} = iJ_y H_{v\tilde{v}}^{(1)} + H_{v\tilde{v}}^{(1)} iJ_y + \{J_x, J_z\}_+ H_{v\tilde{v}}^{(2)} + H_{v\tilde{v}}^{(2)}\{J_x, J_z\}_+ + \ldots \tag{5}$$

Finally, when $\Gamma = A_2$, a Coriolis interaction of the following type is possible

$$H_{v\tilde{v}} = iJ_x H_{v\tilde{v}}^{(1)} + H_{v\tilde{v}}^{(1)} iJ_x + \{J_y, J_z\}_+ H_{v\tilde{v}}^{(2)} + H_{v\tilde{v}}^{(2)}\{J_y, J_z\}_+ \ldots \tag{6}$$

The operators $H_{v\tilde{v}}^{(i)}$, $i = 1, 2, 3, \ldots$ in eqs 4−6 have the form

$$H_{v\tilde{v}}^{(i)} = \frac{1}{2}{}^{v\tilde{v}}C^i + {}^{v\tilde{v}}C_K^i J_z^2 + \frac{1}{2}{}^{v\tilde{v}}C_J^i J^2 + \ldots \tag{7}$$

These equations are used in the rovibrational analysis, which was necessary in the assignment procedure.

The information derived from the rovibrational analysis providing effective Hamiltonian parameters can be considered to be the first step toward the determination of an empirical multidimensional potential hypersurface of methane. The small experimental uncertainty (estimated to be between 0.0001 and 0.001 $cm^{-1}$ for different bands and different spectral regions and always below 0.01 $cm^{-1}$) of the numerous band centers allowed us to correctly determine the values of the harmonic wavenumbers $\omega_k$, anharmonic coefficients $x_{kj}$, and of some resonance interaction parameters. A total of 74 band centers derived in the present contribution (71 new and 3 redetermined for the bands $2\nu_3$, $\nu_1$, and $\nu_6$) were added to the 19 band centers known previously from refs 46, 47, 57, 59, and 60and fitted with the simple model of a vibrational Hamiltonian matrix which takes into account some relevant resonance interactions

$$H^{v.} = \sum_{v,\tilde{v}} |v\rangle\langle\tilde{v}| h_{v\tilde{v}} \tag{8}$$

Here the summation includes all vibrational states studied. The diagonal elements of the matrix have the form

$$h_{vv} = \sum_k \omega_k\left(v_k + \frac{1}{2}\right) + \sum_{k,m\geq k} x_{km}\left(v_k + \frac{1}{2}\right)\left(v_m + \frac{1}{2}\right) + \sum_{k,m\geq k,n\geq m} y_{kmn}\left(v_k + \frac{1}{2}\right)\left(v_m + \frac{1}{2}\right)\left(v_n + \frac{1}{2}\right) \tag{9}$$

Concerning resonance interaction matrix elements, it was found that the following types are important for the current

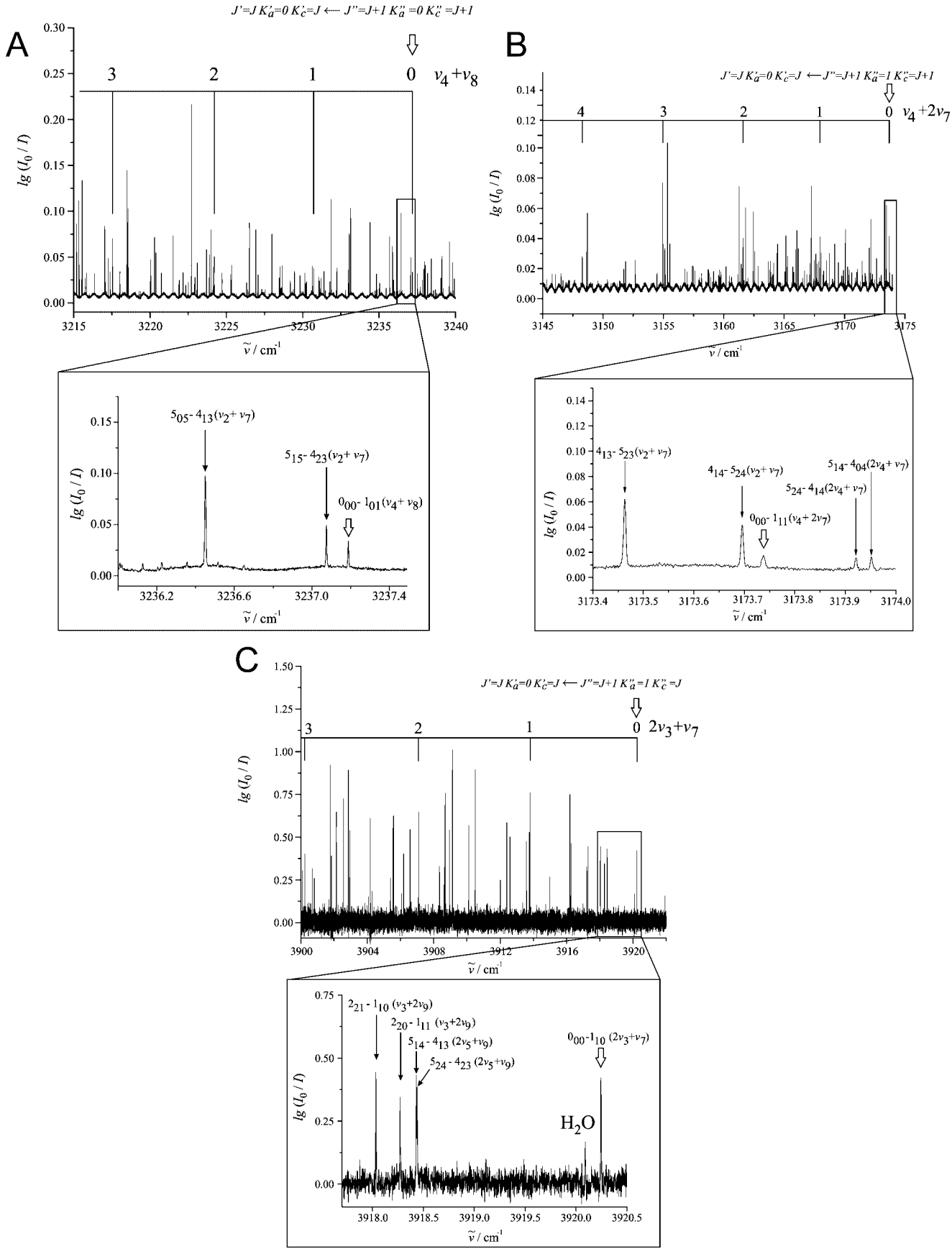


**Figure 6.** Set of transitions $[J', K_a' = 0, K_c' = J'](\upsilon') \leftarrow [J'' = J' + 1, K_a'' = 0/1, K_c'' = J' + 1/J'](\upsilon'' = 0)$ for the bands of different symmetry: (a) *a*-type transitions for the $B_2$-symmetry upper vibrational state (the lower is the ground vibrational state of the $A_1$-symmetry); (b) *b*-type transitions for the $A_1$-symmetry upper state; (c) *c*-type transitions for the $B_1$-symmetry upper state. The first line of progressions, which corresponds the transitions with $J' = 0$, can be recognized beyond doubt. Alternation of the stronger and weaker lines in the set is caused by the nuclear spin statistic of rotational levels. The lower parts of the Figures 6a−6c show in more detail the sections of the spectra close to the transition $[J' = 0, K_a' = 0, K_c' = 0](\upsilon') \leftarrow [J'' = 1, K_a'' = 0/1, K_c'' = 1/0](\upsilon'')$. Assigned lines of some other bands also indicated.

**TABLE 4: Ground State Rotational Parameters (in $cm^{-1}$) for $CH_2D_2$ Obtained from Ground-State Combination Differences (GSCD) of the Present Study**

| parameter | present study | from ref 47 |
|---|---|---|
| 1 | 2 | 3 |
| $A$ | 4.3028927(25)[c] | 4.3028950 |
| $B$ | 3.5059459(24) | 3.5059379 |
| $C$ | 3.0500947(22) | 3.0500936 |
| $\Delta_K/10^{-4}$ | 0.74406(150) | 0.741677 |
| $\Delta_{JK}/10^{-4}$ | −0.15861(147) | −0.153933 |
| $\Delta_J/10^{-4}$ | 0.470106(405) | 0.468558 |
| $\delta_K/10^{-4}$ | −0.15729(167) | −0.158331 |
| $\delta_J/10^{-4}$ | 0.090279(252) | 0.089864 |
| $H_K/10^{-8}$ | −0.104214[b] | −0.104214 |
| $H_{KJ}/10^{-8}$ | 0.94465[b] | 0.94465 |
| $H_{JK}/10^{-8}$ | −0.34124[b] | −0.34124 |
| $H_J/10^{-8}$ | 0.181618[b] | 0.181618 |
| $h_K/10^{-8}$ | 0.34986[b] | 0.34986 |
| $h_{JK}/10^{-8}$ | −0.25873[b] | −0.25873 |
| $h_J/10^{-8}$ | 0.069674[b] | 0.069674 |
| $N$[a] | 134 | 134 |
| $n$[a] | 8 | |
| $d_{rms}$ | 0.000066 | 0.000071 |

[a] Here $N$ is the number of GSCD used in the fit; $n$ is the number of varied parameters. [b] Constrained to the value from column 3. [c] Uncertainties are given in parentheses in terms of one standard deviation in units of the last digits given.

problem and should be taken into account in defining the parameters of the effective Hamiltonian to be reported below.

1. (first type)

$$h_{v\tilde{v}} = \frac{\gamma_{3499}}{8}(2v_3 \pm 1 + 1)^{1/2}(2v_4 \pm 1 + 1)^{1/2}(v_9 \mp 1 + 1)^{1/2}(v_9 \mp 1)^{1/2} \quad (10)$$

if $|v\rangle = (..., v_3, v_4, ..., v_9)$ and $|\tilde{v}\rangle = (..., v_3 \pm 1, v_4 \pm 1, ..., v_9 \mp 2)$;

2. (second type)

$$h_{v\tilde{v}} = \frac{1}{4}(2v_2 \pm 1 + 1)^{1/2}(v_7 \mp 1 + 1)^{1/2}(v_7 \mp 1)^{1/2}(k_{277} + \delta_{277}(2v_7 \mp 2 + 1)) \quad (11)$$

if $|v\rangle = (..., v_2, ..., v_7, ...)$ and $|\tilde{v}\rangle = (..., v_2 \pm 1, ..., v_7 \mp 2, ...)$;

3. (third type)

$$h_{v\tilde{v}} = \frac{k_{489}}{8}(2v_8 \pm 1 + 1)^{1/2}(2v_4 \mp 1 + 1)^{1/2}(2v_9 \mp 1 + 1)^{1/2} \quad (12)$$

if $|v\rangle = (..., v_4, ..., v_8, v_9)$ and $|\tilde{v}\rangle = (..., v_4 \mp 1, ..., v_8 \pm 1, v_9 \mp 1)$;

4. (fourth type)

$$h_{v\tilde{v}} = \frac{k_{133}}{4}(2v_1 \pm 1 + 1)^{1/2}(v_3 \mp 1 + 1)^{1/2}(v_3 \mp 1)^{1/2} \quad (13)$$

if $|v\rangle = (v_1, ..., v_3, ...)$ and $|\tilde{v}\rangle = (v_1 \pm 1, ..., v_3 \mp 2, ...)$;

5. (fifth type)

$$h_{v\tilde{v}} = \frac{\gamma_{3759}}{16}(2v_3 \pm 1 + 1)^{1/2}(2v_7 \pm 1 + 1)^{1/2}(2v_5 \mp 1 + 1)^{1/2}(2v_9 \mp 1 + 1)^{1/2} \quad (14)$$

if $|v\rangle = (..., v_3, ..., v_5, ..., v_7, ..., v_9)$ and $|\tilde{v}\rangle = (..., v_3 \pm 1, ..., v_5 \mp 2, ..., v_7 \pm 1, ..., v_9 \mp 1)$;

6. (sixth type)

$$h_{v\tilde{v}} = \frac{\gamma_{1166}}{4}(v_1 \pm 1 + 1)^{1/2}(v_1 \pm 1)^{1/2}(v_6 \mp 1 + 1)^{1/2}(v_6 \mp 1)^{1/2} \quad (15)$$

if $|v\rangle = (v_1, ..., v_6, ...)$ and $|\tilde{v}\rangle = (v_1 \pm 2, ..., v_6 \mp 2, ...)$.

Those quantum numbers $v_i$, which are not mentioned in eqs 10−15, have the same values in both of the states $|v\rangle$ and $|\tilde{v}\rangle$.

## 5. Results of the Final Analysis and Discussion

In the final calculation, a set of 47 parameters were adjusted in a least-squares analysis. The values obtained are presented in columns 2 of Tables 6 and 7 together with their statistical confidence intervals ($1\sigma$). The parameters reproduce the experimental values of the band centers used in the fit with a root-mean-square deviation $d_{rms} = 0.67$ $cm^{-1}$. Columns 3 of Tables 6 and 7 present, for comparison, also the corresponding ab initio data from ref 83. In column 3 of Table 5, the values of the band centers calculated with the parameters from columns 2 of Tables 6 and 7 are listed. There is in general excellent agreement between the experimental and calculated values of the band centers. The root-mean-square deviation of the fit is 0.67 $cm^{-1}$, with few differences being larger than 1 $cm^{-1}$ and none larger than 2 $cm^{-1}$ for the 89 fitted bands.

Some points are noteworthy in the context of the fit. First, in the fit procedure we did not adjust the harmonic wavenumbers $\omega_k$ ($k = 1, ..., 9$), but instead we determined the parameters $F_{ij}$ of the harmonic force field as defined by[3,35,84]

$$2V^{(2)} = F_{11}S_1^2 + F_{22}(S_{2a}^2 + S_{2b}^2) + F_{33}(S_{3x}^2 + S_{3y}^2 + S_{3z}^2) + 2F_{34}(S_{3x}S_{4x} + S_{3y}S_{4y} + S_{3z}S_{4z}) + F_{44}(S_{4x}^2 + S_{4y}^2 + S_{4z}^2) \quad (16)$$

for methane, because for a given $r_e$-structure[46,47] the nine harmonic wavenumbers $\omega_k$ are exactly described by the five force constants $F_{ij}$ of eq 16. This smaller set of parameters was thus used in the fit.

Second, some of the $x_{kl}$ and $F_{ij}$ turn out to be unstable in the fit to the set of available experimental band centers. The confidence intervals of some parameters were found to be comparable with or even larger than the absolute values of parameters themselves. These parameters were therefore constrained to the values predicted on the basis of a preliminary estimate of the "experimental" potential energy surface of the methane molecule, refs 80 and 83, and were not fitted. The corresponding values are given in Tables 6 and 7 without confidence intervals.

The centers of the four bands $\nu_4 + \nu_7 + \nu_9$, $\nu_3 + \nu_7 + \nu_9$, $\nu_5 + \nu_6$, and $\nu_5 + \nu_8$ were not included in the fit as discussed above. These values as given in column 3 of Table 5 are thus predictions, showing a good predictive power of the simple model at least for these bands. One can compare also with the band centers predicted using the parameters from the ab initio calculations of ref 83. Here many of the predicted values are quite different from the experimental result and from our model. The discrepancies frequently exceed 20 $cm^{-1}$ and more. When one looks more closely into the details of the discrepancies, one finds that while the CH-stretching fundamentals $\nu_1$ and $\nu_6$ are rather well described by the ab initio theory of 83 the CD-stretching fundamentals $\nu_2$ and $\nu_8$ show discrepancies on the order of 10−20 $cm^{-1}$. It is thus not surprising that more highly excited levels involving CD-stretching excitations are incorrectly predicted by ab initio theory. The discrepancies do obviously not arise from the harmonic force field, as experimental and theoretical harmonic wavenumbers in Table 7 agree well. Indeed, our experimental results for the harmonic frequencies agree much better with the ab initio theory of Lee, Martin, and Taylor[83] than with the experimental result of Gray and Robiette,[85] which for a long time constituted the best experimental result but is now

**TABLE 5: Values of the Band Centers of the $CH_2D_2$ Molecule (in $cm^{-1}$)[a]**

| band | center[83] | center, calc. | center, exp. | ref | band | center[83] | center, calc. | center, exp. | ref |
|---|---|---|---|---|---|---|---|---|---|
| 1 | 2 | 3 | 4 | 5 | 1 | 2 | 3 | 4 | 5 |
| $\nu_4, A_1$ | 1033.89 | 1032.18 | 1033.053 | 59 | $\nu_3 + \nu_4 + \nu_9, B_2$ | 3702.14 | 3718.76 | 3719.5909 | tw |
| $\nu_7, B_1$ | 1093.49 | 1090.33 | 1091.185 | 59 | $2\nu_5 + \nu_7, B_1$ | 3751.29 | 3748.78 | 3748.3253 | tw |
| $\nu_9, B_2$ | 1235.31 | 1236.87 | 1236.277 | 59 | $\nu_3 + \nu_7 + \nu_9, A_2$ | 3761.25 | 3749.11 | 3749.0[b] | tw |
| $\nu_5, A_2$ | 1330.73 | 1331.49 | 1331.409 | 47 | $\nu_5 + 2\nu_9, A_2$ | 3775.14 | 3781.97 | | |
| $\nu_3, A_1$ | 1435.72 | 1434.84 | 1435.135 | 59 | $\nu_3 + \nu_4 + \nu_5, A_2$ | 3798.88 | 3798.88 | | |
| $2\nu_4, A_1$ | 2058.80 | 2053.94 | 2054.163 | 60 | $\nu_3 + \nu_5 + \nu_7, B_2$ | 3852.36 | 3842.95 | 3842.4298 | tw |
| $\nu_4 + \nu_7, B_1$ | 2128.11 | 2121.63 | 2124.678 | 60 | $2\nu_3 + \nu_4, A_1$ | 3888.82 | 3880.88 | 3881.0299 | tw |
| $\nu_2, A_1$ | 2167.65 | 2145.76 | 2145.692 | 60 | $2\nu_5 + \nu_9, B_2$ | 3874.83 | 3881.55 | 3882.0088 | tw |
| $2\nu_7, A_1$ | 2183.22 | 2203.39 | 2203.217 | 60 | $\nu_3 + 2\nu_9, A_1$ | 3898.96 | 3900.47 | | |
| $\nu_8, B_2$ | 2246.64 | 2235.53 | 2234.692 | 60 | $2\nu_3 + \nu_7, B_1$ | 3936.44 | 3928.25 | 3928.0540 | tw |
| $\nu_4 + \nu_9, B_2$ | 2267.29 | 2285.55 | 2285.977 | 60 | $3\nu_5, A_2$ | 3978.91 | 3978.59 | | |
| $\nu_7 + \nu_9, A_2$ | 2332.39 | 2329.66 | 2329.698 | 47 | $\nu_3 + \nu_5 + \nu_9, B_1$ | 3993.23 | 3995.88 | 3996.0063 | tw |
| $\nu_4 + \nu_5, A_2$ | 2365.13 | 2365.14 | | | $\nu_1 + \nu_4, A_1$ | 4003.91 | 4005.23 | 4005.6345 | tw |
| $\nu_5 + \nu_7, B_2$ | 2424.60 | 2422.20 | 2422.025 | 46 | $\nu_4 + \nu_6, B_1$ | 4040.50 | 4043.07 | 4042.5767 | tw |
| $2\nu_9, A_1$ | 2461.92 | 2459.14 | 2458.794 | 46 | $\nu_1 + \nu_7, B_1$ | 4056.77 | 4057.95 | 4057.5764 | tw |
| $\nu_3 + \nu_4, A_1$ | 2468.09 | 2469.13 | 2469.201 | 46 | $4\nu_4, A_1$ | 4081.66 | 4066.23 | | |
| $\nu_3 + \nu_7, B_1$ | 2521.70 | 2515.49 | 2515.449 | 46 | $\nu_6 + \nu_7, A_1$ | 4090.24 | 4091.29 | 4092.0424 | tw |
| $\nu_5 + \nu_9, B_1$ | 2557.29 | 2561.06 | 2560.547 | 46 | $\nu_3 + 2\nu_5, A_1$ | 4091.88 | 4091.64 | | |
| $2\nu_5, A_1$ | 2657.04 | 2657.69 | 2658.335 | 57 | $2\nu_3 + \nu_9, B_2$ | 4094.63 | 4091.90 | 4091.0094 | tw |
| $\nu_3 + \nu_9, B_2$ | 2671.70 | 2671.53 | 2671.684 | 57 | $3\nu_4 + \nu_7, B_1$ | 4170.40 | 4153.01 | | |
| $\nu_3 + \nu_5, A_2$ | 2766.02 | 2766.89 | | | $2\nu_3 + \nu_5, A_2$ | 4187.84 | 4185.61 | | |
| $2\nu_3, A_1$ | 2858.01 | 2855.40 | 2855.6650 | tw | $\nu_2 + 2\nu_4, A_1$ | 4228.15 | 4197.33 | 4197.2292 | tw |
| $\nu_1, A_1$ | 2972.07 | 2975.51 | 2975.4823 | tw | $\nu_1 + \nu_9, B_2$ | 4201.24 | 4211.77 | | |
| $\nu_6, B_1$ | 3008.02 | 3012.03 | 3012.2595 | tw | $\nu_6 + \nu_9, A_2$ | 4232.52 | 4236.17 | | |
| $3\nu_4, A_1$ | 3074.72 | 3065.29 | 3066.1341 | tw | $\nu_2 + \nu_4 + \nu_7, B_1$ | 4288.60 | 4240.96 | | |
| $2\nu_4 + \nu_7, B_1$ | 3153.74 | 3142.53 | 3141.6263 | tw | $2\nu_4 + \nu_8, B_2$ | 4274.20 | 4242.94 | 4243.9468 | tw |
| $\nu_2 + \nu_4, A_1$ | 3202.39 | 3182.76 | 3183.6831 | tw | $2\nu_4 + 2\nu_7, A_1$ | 4244.93 | 4255.09 | | |
| $\nu_2 + \nu_7, B_1$ | 3253.12 | 3210.87 | 3210.2675 | tw | $3\nu_3, A_1$ | 4307.05 | 4262.77 | 4263.0639 | tw |
| $\nu_4 + 2\nu_7, A_1$ | 3253.13 | 3234.44 | 3233.6809 | tw | $2\nu_2, A_1$ | 4266.81 | 4263.02 | 4263.2818 | tw |
| $2\nu_4 + \nu_9, B_2$ | 3264.92 | 3243.30 | 3243.7448 | tw | $\nu_1 + \nu_5, A_2$ | 4291.05 | 4295.64 | | |
| $3\nu_7, B_1$ | 3269.19 | 3306.81 | 3306.7646 | tw | $\nu_2 + \nu_4 + \nu_9, B_2$ | 4431.45 | 4328.82 | 4327.2766 | tw |
| $\nu_4 + \nu_8, B_2$ | 3290.29 | 3313.54 | 3313.6709 | tw | $\nu_4 + \nu_7 + \nu_8, A_2$ | 4352.13 | 4328.92 | | |
| $\nu_7 + \nu_8, A_2$ | 3333.13 | 3320.80 | | | $\nu_2 + 2\nu_7, A_1$ | 4334.84 | 4331.53 | | |
| $\nu_4 + \nu_7 + \nu_9, A_2$ | 3365.10 | 3374.53 | 3375.9[b] | tw | $\nu_5 + \nu_6, B_2$ | 4325.88 | 4331.60 | 4332.0[b] | tw |
| $\nu_2 + \nu_9, B_2$ | 3398.63 | 3380.82 | 3381.4722 | tw | $\nu_4 + 3\nu_7, B_1$ | 4305.27 | 4337.04 | | |
| $2\nu_4 + \nu_5, A_2$ | 3390.55 | 3388.37 | | | $\nu_2 + \nu_8, B_2$ | 4354.57 | 4348.15 | 4348.1006 | tw |
| $2\nu_7 + \nu_9, B_2$ | 3425.71 | 3439.33 | 3439.4943 | tw | $3\nu_4 + \nu_5, A_2$ | 4407.00 | 4401.05 | | |
| $\nu_4 + 2\nu_9, A_1$ | 3466.34 | 3451.08 | 3449.1771 | tw | $2\nu_4 + \nu_7 + \nu_9, A_2$ | 4388.82 | 4401.57 | | |
| $\nu_4 + \nu_5 + \nu_7, B_2$ | 3459.73 | 3454.98 | | | $\nu_1 + \nu_3, A_1$ | 4400.55 | 4401.81 | | |
| $\nu_2 + \nu_5, A_2$ | 3491.06 | 3473.85 | | | $2\nu_7 + \nu_8, B_2$ | 4415.86 | 4412.40 | 4413.7498 | tw |
| $\nu_3 + 2\nu_4, A_1$ | 3491.46 | 3484.72 | 3484.3728 | tw | $4\nu_7, A_1$ | 435141 | 4415.75 | | |
| $\nu_8 + \nu_9, A_1$ | 3491.99 | 3521.63 | 3522.1169 | tw | $3\nu_4 + \nu_9, B_2$ | 4304..29 | 4423.72 | | |
| $\nu_5 + 2\nu_7, A_2$ | 3514.72 | 3531.73 | | | $\nu_3 + \nu_6, B_1$ | 4421.61 | 4425.36 | 4425.5493 | tw |
| $\nu_3 + \nu_4 + \nu_7, B_1$ | 3554.78 | 3542.35 | | | $\nu_4 + \nu_8 + \nu_9, A_1$ | 4482.70 | 4435.43 | 4436.4881 | tw |
| $\nu_7 + 2\nu_9, B_1$ | 3562.59 | 3558.11 | | | $\nu_2 + \nu_7 + \nu_9, A_2$ | 4487.69 | 4449.14 | | |
| $\nu_5 + \nu_8, B_1$ | 3567.72 | 3562.07 | 3561.3[b] | tw | $2\nu_4 + \nu_5 + \nu_7, B_2$ | 4485.88 | 4477.31 | | |
| $\nu_2 + \nu_3, A_1$ | 3603.90 | 3569.23 | 3569.6894 | tw | $\nu_4 + 2\nu_7 + \nu_9, B_2$ | 4459.15 | 4479.11 | | |
| $\nu_4 + \nu_5 + \nu_9, B_1$ | 3589.78 | 3609.36 | 3609.7748 | tw | $2\nu_8, A_1$ | 4456.12 | 4485.57 | 4485.2623 | tw |
| $\nu_3 + 2\nu_7, A_1$ | 3601.33 | 3626.93 | 3626.6605 | tw | $\nu_3 + 3\nu_4, A_1$ | 4505.84 | 4496.89 | 4496.5313 | tw |
| $\nu_5 + \nu_7 + \nu_9, A1$ | 3654.73 | 3656.33 | | | $\nu_2 + \nu_4 + \nu_5, A_2$ | 4526.31 | 4506.40 | | |
| $\nu_3 + \nu_8, B_2$ | 3679.31 | 3665.11 | 3663.8061 | tw | $\nu_2 + \nu_5 + \nu_7, B_2$ | 4576.92 | 4539.76 | | |
| $3\nu_9, B_2$ | 3679.82 | 3679.92 | 3680.0021 | tw | $\nu_7 + \nu_8 + \nu_9, B_1$ | 4556.42 | 4540.28 | 4539.7954 | tw |
| $\nu_4 + 2\nu_5, A_1$ | 3691.94 | 3692.80 | 3692.5422 | tw | $3\nu_7 + \nu_9, A_2$ | 4515.28 | 4544.47 | | |
| $\nu_2 + 2\nu_9, A_1$ | 4620.89 | 4558.21 | 4557.8901 | tw | $3\nu_5 + \nu_7, B_2$ | 5073.56 | 5070.07 | | |
| $\nu_3 + 2\nu_4 + \nu_7, B_1$ | 4578.87 | 4560.06 | | | $2\nu_3 + \nu_8, B_2$ | 5098.52 | 5082.69 | | |
| $\nu_4 + \nu_5 + 2\nu_7, A_2$ | 4550.58 | 4564.18 | | | $\nu_1 + \nu_4 + \nu_7, B_1$ | 5089.34 | 5086.82 | | |
| $\nu_4 + \nu_5 + \nu_8, B_1$ | 4586.50 | 4572.48 | | | $2\nu_5 + 2\nu_9, A_1$ | 5083.93 | 5101.94 | | |
| $2\nu_4 + 2\nu_9, A_1$ | 4513.07 | 4595.48 | | | $\nu_1 + 2\nu_7, A_1$ | 5137.71 | 5111.12 | 5111.5773 | tw |
| $\nu_3 + \nu_4 + 2\nu_7, A_1$ | 4637.71 | 4606.41 | | | $\nu_3 + 3\nu_9, B_2$ | 5117.51 | 5111.35 | | |
| $\nu_4 + \nu_7 + 2\nu_9, B_1$ | 4593.38 | 4612.33 | | | $\nu_4 + \nu_6 + \nu_7, A_1$ | 5123.44 | 5121.46 | | |
| $2\nu_4 + \nu_5 + \nu_9, B_1$ | 4613.28 | 4625.58 | | | $\nu_3 + \nu_4 + 2\nu_5, A_1$ | 5125.25 | 5125.52 | | |
| $\nu_5 + 3\nu_7, B_2$ | 4601.08 | 4635.12 | | | $2\nu_3 + \nu_4 + \nu_9, B_2$ | 5123.52 | 5139.04 | | |
| $\nu_2 + \nu_3 + \nu_7, B_1$ | 4679.27 | 4638.63 | | | $\nu_6 + 2\nu_7, B_1$ | 5168.70 | 5144.12 | 5142.7189 | tw |
| $2\nu_7 + 2\nu_9, A_1$ | 4659.51 | 4643.77 | | | $4\nu_4 + \nu_7, B_1$ | 5178.06 | 5153.08 | | |
| $\nu_8 + 2\nu_9, B_2$ | 4677.33 | 4655.55 | | | $2\nu_3 + \nu_7 + \nu_9, A_2$ | 5176.65 | 5161.80 | | |
| $\nu_5 + \nu_7 + \nu_8, A_1$ | 4654.59 | 4657.08 | | | $\nu_3 + 2\nu_5 + \nu_7, B_1$ | 5178.61 | 5162.58 | | |
| $\nu_4 + 3\nu_9, B_2$ | 4707.97 | 4676.48 | | | $\nu_1 + \nu_2, A_1$ | 5138.89 | 5170.18 | 5169.8626 | tw |
| $\nu_2 + \nu_3 + \nu_4, A_1$ | 4634.53 | 4668.22 | 4668.2418 | tw | $3\nu_5 + \nu_9, B_1$ | 5187.96 | 5199.29 | | |
| $\nu_4 + \nu_5 + \nu_7 + \nu_9, A_1$ | 4687.97 | 4700.07 | | | $\nu_1 + \nu_8, B_2$ | 5219.11 | 5204.04 | 5204.9991 | tw |
| $\nu_3 + 3\nu_7, B_1$ | 4682.34 | 4700.74 | | | $\nu_2 + \nu_6, B_1$ | 5175.17 | 5206.44 | 5206.9582 | tw |

**TABLE 5 Continued**

| band | center[83] | center, calc. | center, exp. | ref | band | center[83] | center, calc. | center, exp. | ref |
|---|---|---|---|---|---|---|---|---|---|
| 1 | 2 | 3 | 4 | 5 | 1 | 2 | 3 | 4 | 5 |
| $2\nu_4 + 2\nu_5, A_1$ | 4717.88 | 4717.51 | | | $\nu_2 + 3\nu_4, A_1$ | 5244.92 | 5207.48 | | |
| $\nu_2 + \nu_5 + \nu_9, B_1$ | 4713.27 | 4721.39 | | | $\nu_3 + \nu_5 + 2\nu_9, A_2$ | 5211.73 | 5210.12 | | |
| $\nu_3 + \nu_4 + \nu_8, B_2$ | 4696.04 | 4734.85 | 4736.0100 | tw | $2\nu_3 + \nu_4 + \nu_5, A_2$ | 5219.17 | 5222.97 | | |
| $\nu_3 + \nu_7 + \nu_8, A_2$ | 4758.27 | 4739.87 | | | $3\nu_4 + \nu_8, B_2$ | 5274.51 | 5233.34 | | |
| $\nu_3 + 2\nu_4 + \nu_9, B_2$ | 4723.59 | 4752.70 | | | $\nu_6 + \nu_8, A_2$ | 5258.38 | 5243.03 | | |
| $\nu_5 + 2\nu_7 + \nu_9, B_1$ | 4748.46 | 4764.05 | | | $2\nu_3 + \nu_5 + \nu_7, B_2$ | 5266.65 | 5254.67 | | |
| $\nu_5 + \nu_8 + \nu_9, A_2$ | 4778.65 | 4768.97 | | | $\nu_1 + \nu_4 + \nu_9, B_2$ | 5231.17 | 5255.85 | 5256.4396 | tw |
| $\nu_7 + 3\nu_9, A_2$ | 4784.08 | 4775.23 | | | $\nu_2 + 2\nu_4 + \nu_7, B_1$ | 5315.08 | 5260.63 | | |
| $\nu_4 + 2\nu_5 + \nu_7, B_1$ | 4786.93 | 4783.03 | | | $3\nu_4 + 2\nu_7, A_1$ | 5262.31 | 5265.34 | | |
| $\nu_2 + 2\nu_5, A_1$ | 4810.05 | 4796.09 | | | $3\nu_3 + \nu_4, A_1$ | 5296.09 | 5286.90 | | |
| $\nu_3 + \nu_4 + \nu_7 + \nu_9, A_2$ | 4792.42 | 4797.87 | | | $\nu_4 + \nu_6 + \nu_9, A_2$ | 5263.08 | 5291.96 | | |
| $\nu_3 + 2\nu_7 + \nu_9, B_2$ | 4847.04 | 4803.60 | | | $2\nu_2 + \nu_4, A_1$ | 5342.64 | 5292.64 | | |
| $\nu_4 + \nu_5 + 2\nu_9, A_2$ | 4805.72 | 4817.97 | | | $4\nu_5, A_1$ | 5296.38 | 5294.19 | | |
| $\nu_3 + 2\nu_4 + \nu_5, A_2$ | 4822.76 | 4839.42 | | | $\nu_1 + \nu_7 + \nu_9, A_2$ | 5289.53 | 5296.72 | | |
| $\nu_2 + \nu_3 + \nu_9, B_2$ | 4832.94 | 4854.31 | 4854.4146 | tw | $\nu_3 + 2\nu_5 + \nu_9, B_2$ | 5310.33 | 5316.05 | | |
| $2\nu_5 + 2\nu_7, A_1$ | 4841.80 | 4855.34 | | | $\nu_6 + \nu_7 + \nu_9, B_2$ | 5318.32 | 5317.89 | 5318.5860 | tw |
| $\nu_5 + \nu_7 + 2\nu_9, B_2$ | 4876.19 | 4867.60 | | | $2\nu_3 + 2\nu_9, A_1$ | 5322.53 | 5320.08 | | |
| $4\nu_9, A_1$ | 4889.01 | 4874.38 | | | $\nu_1 + \nu_4 + \nu_5, A_2$ | 5323.39 | 5326.82 | | |
| $2\nu_5 + \nu_8, B_2$ | 4884.37 | 4881.50 | | | $2\nu_4 + \nu_7 + \nu_8, A_2$ | 5362.15 | 5327.76 | | |
| $\nu_3 + \nu_4 + \nu_5 + \nu_7, B_2$ | 4885.95 | 4887.49 | | | $3\nu_3 + \nu_7, B_1$ | 5337.72 | 5328.21 | | |
| $\nu_3 + \nu_4 + 2\nu_9, A_1$ | 4927.48 | 4889.93 | | | $4\nu_4 + \nu_9, B_2$ | 5309.32 | 5332.51 | | |
| $\nu_2 + \nu_3 + \nu_5, A_2$ | 4924.28 | 4895.98 | | | $2\nu_4 + 3\nu_7, B_1$ | 5332.35 | 5353.10 | | |
| $2\nu_3 + 2\nu_4, A_1$ | 4910.65 | 4902.61 | | | $2\nu_2 + \nu_7, B_1$ | 5384.50 | 5356.85 | | |
| $\nu_4 + 2\nu_5 + \nu_9, B_2$ | 4907.84 | 4928.61 | | | $\nu_2 + \nu_4 + \nu_8, B_2$ | 5373.68 | 5356.95 | | |
| $\nu_3 + \nu_5 + 2\nu_7, A_2$ | 4934.95 | 4949.22 | | | $\nu_2 + \nu_4 + 2\nu_7, A_1$ | 5371.04 | 5361.90 | | |
| $2\nu_3 + \nu_4 + \nu_7, B_1$ | 4967.98 | 4952.29 | | | $\nu_4 + \nu_5 + \nu_6, B_2$ | 5358.87 | 5364.11 | | |
| $\nu_3 + \nu_8 + \nu_9, A_1$ | 4899.65 | 4954.82 | 4955.2927 | tw | $\nu_1 + \nu_5 + \nu_7, B_2$ | 5376.13 | 5378.54 | | |
| $\nu_5 + 3\nu_9, B_1$ | 4984.29 | 4968.02 | | | $4\nu_4 + \nu_5, A_2$ | 5414.44 | 5403.59 | | |
| $2\nu_3 + 2\nu_7, A_1$ | 5011.11 | 4977.93 | | | $3\nu_4 + \nu_7 + \nu_9, A_2$ | 5403.56 | 5411.08 | | |
| $2\nu_5 + \nu_7 + \nu_9, A_2$ | 4972.68 | 4979.73 | | | $\nu_5 + \nu_6 + \nu_7, A_2$ | 5408.48 | 5411.25 | | |
| $\nu_3 + \nu_7 + 2\nu_9, B_1$ | 4992.10 | 4989.70 | | | $\nu_3 + 3\nu_5, A_2$ | 5413.31 | 5412.09 | | |
| $\nu_3 + \nu_5 + \nu_8, B_1$ | 4999.94 | 5002.36 | | | $\nu_2 + \nu_7 + \nu_8, A_2$ | 5433.03 | 5415.78 | | |
| $\nu_4 + 3\nu_5, A_2$ | 5014.34 | 5015.18 | | | $2\nu_3 + \nu_5 + \nu_9, B_1$ | 5415.70 | 5415.79 | | |
| $\nu_2 + 2\nu_3, A_1$ | 5021.53 | 5024.54 | | | $\nu_4 + 2\nu_8, A_1$ | 5458.77 | 5420.82 | | |
| $\nu_1 + 2\nu_4, A_1$ | 5026.76 | 5039.59 | 5039.5485 | tw | $\nu_4 + 2\nu_7 + \nu_8, B_2$ | 5435.59 | 5422.23 | | |
| $\nu_3 + \nu_4 + \nu_5 + \nu_9, B_1$ | 5024.18 | 5042.37 | | | $\nu_1 + 2\nu_9, A_1$ | 5421.71 | 5427.04 | | |
| $5\nu_4, A_1$ | 5079.62 | 5056.75 | | | $\nu_1 + \nu_3 + \nu_4, A_1$ | 5430.85 | 5439.97 | | |
| $2\nu_4 + \nu_6, B_1$ | 5064.00 | 5063.69 | | | $\nu_4 + 4\nu_7, A_1$ | 5388.21 | 5445.38 | | |
| $\nu_3 + \nu_5 + \nu_7 + \nu_9, A_1$ | 5083.16 | 5064.36 | | | $\nu_2 + 2\nu_4 + \nu_9, B_2$ | 5455.30 | 5446.49 | | |
| $\nu_6 + 2\nu_9, B_1$ | 5448.30 | 5446.68 | 5446.5963 | tw | $\nu_3 + \nu_4 + 3\nu_7, B_1$ | 5716.88 | 5733.46 | | |
| $\nu_3 + \nu_4 + \nu_6, B_1$ | 5452.55 | 5457.54 | | | $\nu_5 + 2\nu_8, A_2$ | 5767.53 | 5738.03 | | |
| $\nu_1 + \nu_3 + \nu_7, B_1$ | 5477.73 | 5474.39 | | | $\nu_5 + 2\nu_7 + \nu_8, B_1$ | 5737.70 | 5742.02 | | |
| $3\nu_7 + \nu_8, A_2$ | 5494.83 | 5484.89 | | | $\nu_5 + 4\nu_7, A_2$ | 5683.68 | 5742.71 | | |
| $2\nu_4 + \nu_8 + \nu_9, A_1$ | 5490.07 | 5486.96 | | | $\nu_3 + \nu_5 + \nu_6, B_2$ | 5739.02 | 5744.49 | | |
| $\nu_2 + 3\nu_7, B_1$ | 5412.80 | 5488.06 | | | $\nu_7 + \nu_8 + 2\nu_9, A_2$ | 5770.99 | 5750.23 | | |
| $3\nu_4 + \nu_5 + \nu_7, B_2$ | 5503.04 | 5489.29 | | | $\nu_2 + \nu_3 + 2\nu_7, A_1$ | 5753.45 | 5750.60 | | |
| $\nu_3 + \nu_6 + \nu_7, A_1$ | 5496.30 | 5495.31 | | | $\nu_2 + \nu_4 + \nu_5 + \nu_9, B_1$ | 5746.61 | 5752.88 | | |
| $2\nu_4 + 2\nu_7 + \nu_9, B_2$ | 5483.59 | 5498.57 | | | $2\nu_4 + 3\nu_9, B_2$ | 5727.13 | 5754.81 | | |
| $3\nu_3 + \nu_9, B_2$ | 5504.08 | 5499.08 | | | $\nu_3 + \nu_4 + \nu_7 + \nu_8, A_2$ | 5775.73 | 5762.15 | | |
| $\nu_3 + 4\nu_4, A_1$ | 5511.24 | 5499.32 | | | $\nu_3 + 3\nu_4 + \nu_9, B_2$ | 5736.08 | 5771.72 | | |
| $2\nu_2 + \nu_9, B_2$ | 5533.67 | 5504.58 | | | $\nu_3 + 4\nu_7, A_1$ | 5757.03 | 5772.22 | | |
| $2\nu_3 + 2\nu_5, A_1$ | 5513.25 | 5510.44 | | | $3\nu_7 + 2\nu_9, B_1$ | 5752.66 | 5773.40 | | |
| $\nu_2 + \nu_4 + \nu_7 + \nu_9, A_2$ | 5521.24 | 5512.01 | | | $\nu_2 + \nu_3 + \nu_8, B_2$ | 5785.16 | 5790.66 | | |
| $\nu_7 + 2\nu_8, B_1$ | 5535.60 | 5519.00 | | | $\nu_4 + \nu_5 + \nu_8 + \nu_9, A_2$ | 5795.52 | 5800.32 | | |
| $\nu_1 + \nu_5 + \nu_9, B_1$ | 5511.46 | 5524.52 | | | $\nu_4 + \nu_5 + 2\nu_7 + \nu_9, B_1$ | 5782.40 | 5803.48 | | |
| $\nu_2 + 2\nu_4 + \nu_5, A_2$ | 5552.58 | 5528.52 | | | $\nu_1 + 2\nu_3, A_1$ | 5815.57 | 5806.56 | 5806.5300 | tw |
| $\nu_5 + \nu_6 + \nu_9, A_1$ | 5541.61 | 5548.09 | 5547.7442 | tw | $2\nu_4 + 2\nu_5 + \nu_7, B_1$ | 5813.60 | 5806.90 | | |
| $\nu_2 + 2\nu_7 + \nu_9, B_2$ | 5572.99 | 5560.85 | | | $\nu_3 + 2\nu_7 + \nu_8, B_2$ | 5833.48 | 5813.70 | | |
| $\nu_2 + \nu_8 + \nu_9, A_1$ | 5569.91 | 5562.51 | 5562.1906 | tw | $\nu_4 + \nu_7 + 3\nu_9, A_2$ | 5812.96 | 5818.82 | | |
| $\nu_4 + \nu_7 + \nu_8 + \nu_9, B_1$ | 5573.50 | 5563.18 | | | $2\nu_3 + \nu_6, B_1$ | 5821.74 | 5819.28 | 5819.1679 | tw |
| $\nu_3 + 3\nu_4 + \nu_7, B_1$ | 5593.98 | 5570.18 | | | $\nu_2 + \nu_5 + \nu_7 + \nu_9, A_1$ | 5802.72 | 5825.01 | | |
| $3\nu_4 + 2\nu_9, A_1$ | 5525.16 | 5578.68 | | | $\nu_2 + 3\nu_9, B_2$ | 5834.44 | 5826.58 | | |
| $2\nu_4 + \nu_5 + \nu_8, B_1$ | 5596.30 | 5579.93 | | | $\nu_3 + 2\nu_4 + \nu_7 + \nu_9, A_2$ | 5814.60 | 5829.99 | | |
| $\nu_4 + 3\nu_7 + \nu_9, A_2$ | 5549.44 | 5581.60 | | | $\nu_2 + \nu_4 + 2\nu_5, A_1$ | 5845.81 | 5830.18 | | |
| $2\nu_4 + \nu_5 + 2\nu_7, A_2$ | 5577.45 | 5586.23 | | | $2\nu_4 + \nu_5 + 2\nu_9, A_2$ | 5827.44 | 5840.97 | | |
| $2\nu_2 + \nu_5, A_2$ | 5623.13 | 5589.16 | | | $\nu_2 + \nu_3 + \nu_4 + \nu_9, B_2$ | 5864.23 | 5846.30 | | |
| $3\nu_3 + \nu_5, A_2$ | 5596.20 | 5592.03 | | | $\nu_8 + 3\nu_9, A_1$ | 5879.60 | 5849.73 | | |
| $\nu_1 + 2\nu_5, A_1$ | 5605.60 | 5610.55 | | | $\nu_3 + 3\nu_4 + \nu_5, A_2$ | 5837.66 | 5860.02 | | |
| $\nu_3 + 2\nu_4 + 2\nu_7, A_1$ | 5662.53 | 5615.01 | | | $\nu_5 + \nu_7 + \nu_8 + \nu_9, B_2$ | 5869.12 | 5860.90 | | |
| $2\nu_8 + \nu_9, B_2$ | 5660.20 | 5630.89 | 5631.3137 | tw | $\nu_2 + 2\nu_5 + \nu_7, B_1$ | 5896.29 | 5863.01 | | |

**TABLE 5 Continued**

| band | center[83] | center, calc. | center, exp. | ref | band | center[83] | center, calc. | center, exp. | ref |
|---|---|---|---|---|---|---|---|---|---|
| 1 | 2 | 3 | 4 | 5 | 1 | 2 | 3 | 4 | 5 |
| $2\nu_7 + \nu_8 + \nu_9$, $A_1$ | 5642.74 | 5634.98 | | | $2\nu_1$, $A_1$ | 5889.44 | 5867.94 | 5867.8242 | tw |
| $\nu_1 + \nu_3 + \nu_9$, $B_2$ | 5630.38 | 5637.91 | | | $\nu_5 + 3\nu_7 + \nu_9$, $A_1$ | 5838.41 | 5870.08 | | |
| $2\nu_5 + \nu_6$, $B_1$ | 5639.32 | 5645.89 | | | $\nu_3 + 2\nu_8$, $A_1$ | 5885.72 | 5870.25 | | |
| $2\nu_4 + \nu_7 + 2\nu_9$, $B_1$ | 5615.19 | 5646.40 | | | $\nu_2 + \nu_3 + \nu_7 + \nu_9$, $A_2$ | 5914.48 | 5875.52 | | |
| $\nu_3 + \nu_6 + \nu_9$, $A_2$ | 5646.75 | 5649.32 | | | $\nu_1 + \nu_6$, $B_1$ | 5865.01 | 5878.56 | 5878.4563 | tw |
| $\nu_2 + \nu_4 + 2\nu_9$, $A_1$ | 5651.80 | 5650.13 | | | $\nu_3 + \nu_4 + 2\nu_7 + \nu_9$, $B_2$ | 5878.94 | 5880.61 | | |
| $3\nu_4 + \nu_5 + \nu_9$, $B_1$ | 5627.80 | 5651.73 | | | $\nu_4 + 2\nu_5 + \nu_8$, $B_2$ | 5903.66 | 5881.36 | | |
| $4\nu_7 + \nu_9$, $B_2$ | 5601.09 | 5653.08 | | | $\nu_4 + 2\nu_5 + 2\nu_7$, $A_1$ | 5878.36 | 5889.17 | | |
| $\nu_2 + \nu_5 + 2\nu_7$, $A_2$ | 5659.02 | 5653.26 | | | $2\nu_7 + 3\nu_9$, $B_2$ | 5884.59 | 5898.84 | | |
| $\nu_2 + \nu_3 + 2\nu_4$, $A_1$ | 5658.74 | 5653.98 | | | $\nu_3 + 2\nu_4 + \nu_5 + \nu_7$, $B_2$ | 5910.56 | 5902.84 | | |
| $\nu_2 + \nu_5 + \nu_8$, $B_1$ | 5668.31 | 5655.35 | | | $\nu_3 + \nu_4 + \nu_8 + \nu_9$, $A_1$ | 5914.47 | 5904.84 | | |
| $4\nu_3$, $A_1$ | 5662.15 | 5657.46 | | | $\nu_2 + \nu_5 + 2\nu_9$, $A_2$ | 5926.79 | 5915.42 | | |
| $\nu_2 + \nu_3 + \nu_4 + \nu_7$, $B_1$ | 5713.20 | 5665.83 | | | $\nu_3 + 2\nu_4 + 2\nu_9$, $A_1$ | 5947.02 | 5921.16 | | |
| $\nu_2 + \nu_4 + \nu_5 + \nu_7$, $B_2$ | 5612.90 | 5666.77 | | | $\nu_3 + 3\nu_7 + \nu_9$, $A_2$ | 5929.08 | 5927.41 | | |
| $\nu_4 + \nu_8 + 2\nu_9$, $B_2$ | 5691.77 | 5671.10 | | | $\nu_4 + \nu_5 + \nu_7 + 2\nu_9$, $B_2$ | 5907.50 | 5933.60 | | |
| $\nu_4 + \nu_5 + \nu_7 + \nu_8$, $A_1$ | 5674.10 | 5673.72 | | | $\nu_5 + \nu_8 + 2\nu_9$, $B_1$ | 5980.88 | 5945.63 | | |
| $\nu_2 + \nu_7 + 2\nu_9$, $B_1$ | 5713.54 | 5677.06 | | | $\nu_2 + \nu_3 + \nu_4 + \nu_5$, $A_2$ | 5958.00 | 5949.38 | | |
| $2\nu_4 + \nu_5 + \nu_7 + \nu_9$, $A_1$ | 5712.20 | 5677.51 | | | $2\nu_4 + 2\nu_5 + \nu_9$, $B_2$ | 5931.86 | 5950.86 | | |
| $\nu_3 + 2\nu_4 + \nu_8$, $B_2$ | 5703.80 | 5705.83 | | | $\nu_4 + 4\nu_9$, $A_1$ | 5915.25 | 5951.66 | | |
| $\nu_4 + 2\nu_7 + 2\nu_9$, $A_1$ | 5691.02 | 5713.89 | | | $2\nu_5 + 3\nu_7$, $B_1$ | 5928.54 | 5958.48 | | |
| $\nu_1 + \nu_3 + \nu_5$, $A_2$ | 5719.08 | 5722.00 | | | $\nu_2 + \nu_3 + \nu_5 + \nu_7$, $B_2$ | 6002.62 | 5958.94 | | |
| $2\nu_2 + \nu_3$, $A_1$ | 5738.65 | 5727.99 | | | $\nu_3 + \nu_4 + \nu_5 + 2\nu_7$, $A_2$ | 5969.27 | 5961.85 | | |
| $3\nu_4 + 2\nu_5$, $A_1$ | 5734.82 | 5731.82 | | | $\nu_3 + \nu_7 + \nu_8 + \nu_9$, $B_1$ | 5982.21 | 5971.18 | | |
| $2\nu_3 + 2\nu_4 + \nu_7$, $B_1$ | 5990.54 | 5975.31 | | | $\nu_3 + \nu_4 + \nu_7 + 2\nu_9$, $B_1$ | 6021.35 | 6026.89 | | |
| $2\nu_5 + \nu_7 + \nu_8$, $A_2$ | 5971.62 | 5984.00 | | | $2\nu_3 + \nu_4 + 2\nu_7$, $A_1$ | 6043.38 | 6027.74 | | |
| $\nu_7 + 4\nu_9$, $B_1$ | 5996.86 | 5986.36 | | | $\nu_2 + 2\nu_3 + \nu_4$, $A_1$ | 6053.19 | 6033.46 | | |
| $2\nu_3 + 3\nu_4$, $A_1$ | 5923.51 | 5992.03 | | | $2\nu_4 + 3\nu_5$, $A_2$ | 6040.79 | 6041.35 | | |
| $\nu_5 + 2\nu_7 + 2\nu_9$, $A_2$ | 5973.49 | 5992.92 | | | $\nu_2 + 2\nu_5 + \nu_9$, $B_2$ | 6023.51 | 6042.11 | | |
| $2\nu_6$, $A_1$ | 5952.76 | 5999.07 | 5998.9646 | tw | $\nu_2 + \nu_3 + 2\nu_9$, $A_1$ | 6055.86 | 6052.32 | | |
| $\nu_4 + \nu_5 + 3\nu_9$, $B_1$ | 6012.95 | 6001.15 | | | $\nu_3 + 2\nu_4 + \nu_5 + \nu_9$, $B_1$ | 6046.15 | 6055.02 | | |
| $\nu_1 + 3\nu_4$, $A_1$ | 6040.63 | 6002.61 | | | $\nu_3 + \nu_5 + \nu_7 + \nu_8$, $A_1$ | 6079.28 | 6064.52 | | |
| $\nu_3 + \nu_5 + 3\nu_7$, $B_2$ | 6013.78 | 6015.46 | | | $2\nu_3 + 3\nu_7$, $B_1$ | 6082.03 | 6073.52 | | |
| $\nu_4 + 2\nu_5 + \nu_7 + \nu_9$, $A_2$ | 6006.48 | 6021.66 | | | $\nu_1 + \nu_4 + \nu_8$, $B_2$ | 6235.33 | 6209.51 | 6208.2925 | tw |
| $\nu_3 + \nu_4 + \nu_5 + \nu_8$, $B_1$ | 6017.18 | 6026.54 | | | $\nu_2 + \nu_6 + \nu_7$, $A_1$ | 6249.37 | 6298.83 | 6298.9003 | tw |

[a] Values presented in column 2 were calculated with the parameters from Tables I (cc-pVQZ) and VI of ref 83. Band centers presented in column 3 were calculated with the parameters from Tables 6 and 7 of the present paper. Experimental values of the band centers are given in column 4. tw (this work) indicates results obtained in the present investigation. [b] Was not used in the fit (see discussion in the text).

**TABLE 6: $F_{ij}$ Parameters of the Methane Molecule**

| parameter | present work | ref 83 | ref 35 |
|---|---|---|---|
| $F_{11}$/aJ Å$^{-2}$ | 5.47384[a] | 5.47384 | 5.43512 |
| $F_{22}$/aJ | 0.578602(332)[b]) | 0.57770 | 0.58401 |
| $F_{33}$/aJ Å$^{-2}$ | 5.387874(832) | 5.37696 | 5.37813 |
| $F_{34}$/aJ Å$^{-1}$ | −0.21057[a] | −0.21057 | −0.22100 |
| $F_{44}$/aJ | 0.533740(416) | 0.53225 | 0.54801 |
| number of experimental band centers | | 89 | |
| number of fitted parameters | | 47 | |
| $d_{rms}$ | | 0.67 cm$^{-1}$ | |

[a] Constrained to the value from ref 83. [b] For uncertainties, see caption to Table 4 and discussion in Section 5.

outdated. The problems of ab initio theory in predicting poorly the experimental band centers therefore reside largely in the anharmonic part of the potential. At this point, one might be tempted to point to the in part large discrepancies between experiment and ab initio theory for the anharmonic constants in Table 7. However, the two sets of constants have a somewhat different physical significance. Whereas the constants of our model are effective Hamiltonian constants obtained from a direct fit to experimental band centers, the anharmonic constants of Lee, Martin, and Taylor are derived from the anharmonic ab initio potential by means of low-order perturbation theory. To compare our anharmonic constants with the ab initio potential of Lee, Martin, and Taylor at the appropriate level of significance, one would have to carry out 9-dimensional vibrational variational calculations on the potential of Lee, Martin, and Taylor and then fit the corresponding calculated band centers (or level positions) with the same effective Hamiltonian as used for the fit to experiment (see also the corresponding discussion in ref 31). The large discrepancies between experimental and theoretical level positions have thus two conceptually quite different origins: They arise

(i) from the errors in the ab initio potential hypersurface and

(ii) from errors in using expressions based on low-order perturbation theory in calculating level positions from anharmonic potential coefficients.

Without carrying out the theoretical program discussed above, it is not easy to separate the different ab initio errors and identify their relative magnitude. Anharmonic constants from the potential of refs 37 and 38 have not been published in detail, thus a direct comparison is not easy. We note, however, that the variational calculations of refs 40−42 on that potential for $\nu_2 + 2\nu_3$ of $CH_4$ differ by more than 10 cm$^{-1}$ from the precise experimental result for this level ($J = 0$, $F_2$ or $F_1^-$ in $S_4^*$ at 7510.3378 ± 0.001 cm$^{-1}$).[65]This thus provides an estimate of the intrinsic errors in that potential.

We might mention here also some simple theoretical models which have been proposed to describe the anharmonic level structure of $CH_2D_2$ in relation to some gas phase[86] and liquid Argon solution experiments.[87] Neither of these is very successful in giving an accurate description. Independent from the theoretical analysis, however, the experimental spectra of $CH_2D_2$ in liquid Argon solution between 94 and 101 K[87] provide an interesting comparison with our low-temperature gas phase spectra in terms of the shifts

**TABLE 7: Vibrational Spectroscopic Parameters of the $CH_2D_2$ Molecule (in $cm^{-1}$)**

| parameter | this work | ref 83 | parameter | this work | ref 83 |
|---|---|---|---|---|---|
| 1 | 2 | 3 | 1 | 2 | 3 |
| $\omega_1$ | 3104.4217[a] | 3102.5 | $x_{38}$ | −3.903(387) | −3.067 |
| $\omega_2$ | 2237.9855[a] | 2236.9 | $x_{39}$ | −0.1829(240) | 0.651 |
| $\omega_3$ | 1472.3115[a] | 1470.9 | $x_{44}$ | −5.207(148) | −4.492 |
| $\omega_4$ | 1054.4405[a] | 1053.1 | $x_{45}$ | 1.4696(165) | 0.512 |
| $\omega_5$ | 1361.2375[a] | 1360.1 | $x_{46}$ | −1.1383(410) | −1.411 |
| $\omega_6$ | 3159.7912[a] | 3156.5 | $x_{47}$ | −0.868(479) | 0.727 |
| $\omega_7$ | 1117.7847[a] | 1116.2 | $x_{48}$ | −15.620[b] | −15.620 |
| $\omega_8$ | 2339.5713[a] | 2337.1 | $x_{49}$ | −2.5710(516) | −1.914 |
| $\omega_9$ | 1267.4576[a] | 1265.7 | $x_{55}$ | −2.648(122) | −2.211 |
| $x_{11}$ | −25.3041(812)[c] | −27.344 | $x_{56}$ | −11.912(248) | −12.869 |
| $x_{12}$ | −3.294(858) | −0.831 | $x_{57}$ | 0.385[b] | 0.385 |
| $x_{13}$ | −15.2348(957) | −7.251 | $x_{58}$ | −9.655[b] | −9.655 |
| $x_{14}$ | −2.4222(828) | −2.052 | $x_{59}$ | −9.6710(420) | −8.755 |
| $x_{15}$ | −11.752[b] | −11.752 | $x_{66}$ | −31.566(151) | −31.640 |
| $x_{16}$ | −114.112(378) | −115.079 | $x_{67}$ | −11.062(496) | −11.273 |
| $x_{17}$ | −7.765(441) | −8.786 | $x_{68}$ | 3.715[b] | 3.715 |
| $x_{18}$ | −9.216(452) | 0.403 | $x_{69}$ | −12.732(178) | −10.822 |
| $x_{19}$ | −0.621(578) | −6.139 | $x_{77}$ | −6.587(602) | −1.879 |
| $x_{22}$ | −10.451(540) | −14.130 | $x_{78}$ | −7.001[b] | −7.001 |
| $x_{23}$ | −3.609(264) | −2.065 | $x_{79}$ | 2.464(468) | 3.590 |
| $x_{24}$ | −0.568(439) | 0.849 | $x_{88}$ | −15.2572(438) | −18.583 |
| $x_{25}$ | −7.320[b] | −7.320 | $x_{89}$ | −9.145(858) | −15.620 |
| $x_{26}$ | −0.509[b] | −0.509 | $x_{99}$ | −5.2575(453) | −4.354 |
| $x_{27}$ | −1.75(158) | −8.016 | $y_{777}$ | 0.6657(525) | - |
| $x_{28}$ | −58.0734(996) | −59.737 | $k_{277}$ | 61.406(207) | - |
| $x_{29}$ | −7.677(392) | −4.344 | $\delta_{277}$ | −1.275(948) | - |
| $x_{33}$ | −5.1914(976) | −6.733 | $k_{489}$ | 68.717(321) | - |
| $x_{34}$ | −1.9829(885) | −1.539 | $\gamma_{3499}$ | 13.888(169) | - |
| $x_{35}$ | −0.447[b] | −0.447 | $k_{133}$ | −42.61(108) | - |
| $x_{36}$ | −21.507(175) | −22.147 | $\gamma_{3759}$ | 40.44(104) | - |
| $x_{37}$ | −7.307(164) | −7.529 | $\gamma_{1166}$ | 124.562(591) | - |

[a] Was not fitted but calculated on the basis of the $F_{ij}$ parameters given in column 2 of Table 6. [b] Constrained to the value from ref 83. [c] Uncertainties are stated in parentheses in terms of one standard deviation of the last digit given (see Section 5).

of the bands in solution in a liquid weakly interacting "rare-gas" solvent compared to the gas phase, the shifts being quite appreciable.

## 6. Conclusions and Outlook

We have demonstrated here that by means of spectra taken with high, Doppler limited resolution at low temperatures around 80 K one can accurately locate a large number of vibrational levels for $CH_2D_2$, using the technique of specific assignment of $J' = 0 \leftarrow J'' = 1$ transitions, which provides pure vibrational level energies. 71 vibrational energies including excitations up to and exceeding 6000 ($hc$) $cm^{-1}$ were thus combined with previously known vibrational band centers to provide a large data set of 93 vibrational energies. An effective Hamiltonian with 47 parameters adjusted to fit these data describes this spectrum with a root-mean-square deviation of less than 0.7 $cm^{-1}$ and no deviations exceeding 2 $cm^{-1}$. A complete list of about 350 levels below 6300 $cm^{-1}$ can thus be accurately calculated and should have good reliability over this whole energy range, extendable by extrapolation to higher energies, at least for heuristic purposes. Indeed, the predicted level positions should be helpful in assigning further vibrational levels in future work. Furthermore one can derive an empirical potential function for methane using these data.[76]

The corresponding level energies in Table 5 can be used as a benchmark for ab initio calculations. For instance, we find that level energies calculated from parameters based on the ab initio calculations of Lee, Martin, and Taylor[83] frequently differ from the experimental results by more than 20 $cm^{-1}$, where the discrepancy arises in part from the ab initio potential and in part from the use of low-order perturbation theoretical expressions in the calculations of ref 83.

In future work, it should also be possible to compare with 9-dimensional vibrational variational calculations similar to those reported for $CH_4$ in refs 40−43 using appropriate full dimensional potential hypersurfaces.[35−38] Adjustment of parameters of such global analytical potentials[35,36] should enable us then to refine the available potentials. These refined potential hypersurfaces can subsequently be used for quantum-dynamical wavepacket calculations, for instance, with coherent infrared multiphoton excitation for various methane isotopomers[34,45] or for accurate calculations of statistical thermodynamical and kinetics properties based on vibrational densities of states in the methane system. Of course, some of these applications can also be directly based on the experimental and empirical effective Hamiltonian results shown in Table 5.

While level positions in Table 5 are accurate, it should be understood that the assignment of normal mode excitations ($\nu_i + \nu_j + \nu_k$) has only an approximate meaning of very limited significance, when there is strong mixing, which we have in fact identified by some of the coupling parameters in Table 6. However, assigned level symmetries are robust and can for instance be used for testing the convergence to symmetry distributions in level densities following.[88] Finally, the present results provide a starting point for a global rovibrational analysis including rovibrational levels to higher $J$-values with extensive anharmonic and Coriolis couplings.[76] Through a combination with similar results for other isotopomers $^{12}CH_4$,[63] $^{13}CH_4$,[64] $CH_3D$, and $CD_3H$,[31,89,90] one can obtain a consistent global description of spectra and dynamics of the stable isotopomers of methane.

**Acknowledgment.** We enjoyed discussion with Fabio Mariotti, Hans Martin Niederer, and Roberto Marquardt. Our work is supported financially by the ETH Zürich and the Schweizerischer Nationalfonds. O.N.U. and E.S.B. are also supported by a PICS grant. We enjoyed many years of friendly scientific exchange with Max Wolfsberg.

## Appendix

**TABLE A1: Lowest Ground-State Combination Differences of the $CH_2D_2$ Molecule (in $cm^{-1}$)[a]**

| | value/$cm^{-1}$ | | $d_{rms}$[a] | | | value/$cm^{-1}$ | | $d_{rms}$[a] | |
|---|---|---|---|---|---|---|---|---|---|
| $J'K'_aK'_c - J''K''_aK''_c$ | fit. | exp.[a] | $10^4$ $cm^{-1}$ | $n$[b] | $J'K'_aK'_c - J''K''_aK''_c$ | fit. | exp.[a] | $10^4$ $cm^{-1}$ | $n$[b] |
| 1 | 2 | 3 | 4 | 5 | 1 | 2 | 3 | 4 | 5 |
| 2 2 0 − 2 0 2 | 4.39224 | 4.39222 | 1.7 | 68 | 5 2 4 − 4 2 2 | 30.79386 | 30.79389 | 1.0 | 62 |
| 3 2 1 − 3 0 3 | 5.40865 | 5.40869 | 1.8 | 81 | 4 2 3 − 3 0 3 | 30.84926 | 30.84928 | 1.1 | 83 |
| 4 3 1 − 4 1 3 | 6.93612 | 6.93615 | 1.8 | 58 | 6 1 6 − 5 1 4 | 31.21071 | 31.21072 | 1.4 | 23 |
| 3 3 0 − 3 1 2 | 7.05255 | 7.05259 | 2.1 | 67 | 3 1 3 − 1 1 1 | 31.55448 | 31.55441 | 1.2 | 51 |
| 4 2 2 − 4 0 4 | 7.26937 | 7.26934 | 1.9 | 53 | 3 0 3 − 1 0 1 | 32.11883 | 32.11880 | 0.8 | 42 |
| 5 3 2 − 5 1 4 | 7.48927 | 7.48924 | 1.2 | 29 | 6 1 5 − 5 3 3 | 32.25480 | 32.25466 | 1.3 | 15 |
| 6 3 3 − 6 1 5 | 8.99002 | 8.99009 | 1.4 | 9 | 5 3 3 − 4 3 1 | 32.81639 | 32.81635 | 1.2 | 60 |
| 6 4 2 − 6 2 4 | 9.58088 | 9.58089 | 1.1 | 10 | 5 4 2 − 4 4 0 | 33.07648 | 33.07667 | 1.8 | 31 |
| 3 3 1 − 3 1 3 | 9.72255 | 9.72255 | 2.2 | 43 | 5 4 1 − 4 5 1 | 33.12952 | 33.12941 | 1.8 | 45 |
| 5 2 3 − 5 0 5 | 9.87175 | 9.87174 | 1.9 | 29 | 4 3 2 − 3 1 2 | 33.45682 | 33.45687 | 1.1 | 77 |
| 5 4 1 − 5 2 3 | 10.13182 | 10.13190 | 1.8 | 32 | 5 3 2 − 4 3 2 | 33.73420 | 33.73414 | 1.4 | 62 |
| 4 4 0 − 4 2 2 | 10.88372 | 10.88369 | 2.3 | 33 | 3 1 2 − 1 1 0 | 33.80009 | 33.80007 | 0.8 | 36 |
| 4 3 2 − 4 1 4 | 11.07795 | 11.07799 | 2.4 | 62 | 5 2 3 − 4 2 3 | 35.51663 | 35.51666 | 1.1 | 57 |
| 2 1 2 − 1 1 0 | 12.19917 | 12.19921 | 1.0 | 71 | 6 2 5 − 5 2 3 | 35.59931 | 35.59930 | 1.2 | 22 |
| 4 4 1 − 4 2 3 | 12.51893 | 12.51889 | 1.7 | 43 | 4 3 1 − 3 1 3 | 36.36331 | 36.36325 | 1.2 | 37 |
| 5 3 3 − 5 1 5 | 12.88537 | 12.88538 | 0.7 | 24 | 5 1 4 − 4 1 4 | 37.32288 | 37.32280 | 1.3 | 73 |
| 5 4 2 − 5 2 4 | 13.16633 | 13.16636 | 1.7 | 27 | 3 2 1 − 1 0 1 | 37.52748 | 37.52754 | 1.0 | 28 |
| 2 1 1 − 1 1 1 | 14.02211 | 14.02210 | 1.7 | 82 | 4 4 1 − 3 2 1 | 37.95954 | 37.95955 | 1.4 | 39 |
| 6 4 3 − 6 2 5 | 14.22886 | 14.22875 | 2.8 | 10 | 5 2 4 − 4 0 4 | 38.06323 | 38.06317 | 1.2 | 53 |
| 6 5 1 − 6 3 3 | 14.38942 | 14.38948 | 1.0 | 8 | 4 4 0 − 3 2 2 | 38.61987 | 38.61986 | 1.5 | 36 |
| 3 0 3 − 2 2 1 | 14.90957 | 14.90955 | 1.5 | 63 | 6 3 4 − 5 3 2 | 38.81953 | 38.81948 | 0.9 | 24 |
| 3 3 0 − 4 1 4 | 15.32632 | 15.32633 | 2.6 | 32 | 6 4 3 − 5 4 1 | 39.69636 | 39.69640 | 0.7 | 15 |
| 5 5 1 − 5 3 3 | 15.94298 | 15.94294 | 0.6 | 12 | 5 3 3 − 4 1 3 | 39.75251 | 39.75246 | 1.3 | 48 |
| 2 2 1 − 1 0 1 | 17.20926 | 17.20924 | 1.6 | 68 | 6 4 2 − 5 4 2 | 39.96171 | 39.96171 | 2.1 | 17 |
| 3 1 3 − 2 1 1 | 17.53237 | 17.53238 | 1.4 | 88 | 4 0 4 − 2 2 0 | 39.98343 | 39.98339 | 1.6 | 13 |
| 3 2 2 − 2 2 0 | 19.51965 | 19.51661 | 1.2 | 80 | 3 3 0 − 1 1 0 | 40.85264 | 40.85270 | 0.8 | 31 |
| 2 0 2 − 0 0 0 | 19.51965 | 19.51974 | 1.3 | 39 | 6 3 3 − 5 3 3 | 41.24482 | 41.24490 | 1.3 | 22 |
| 4 1 3 − 3 3 1 | 19.70464 | 19.70461 | 2.0 | 38 | 3 3 1 − 1 1 1 | 41.27704 | 41.27710 | 0.7 | 30 |
| 5 2 4 − 4 4 0 | 19.91015 | 19.91010 | 1.8 | 12 | 4 4 1 − 3 0 3 | 43.36819 | 43.36816 | 2.2 | 17 |
| 5 1 5 − 4 3 1 | 19.93102 | 19.93101 | 1.7 | 18 | 6 2 4 − 5 2 4 | 43.54716 | 43.54716 | 1.4 | 26 |
| 5 4 1 − 5 0 5 | 20.00356 | 20.00359 | 1.5 | 9 | 5 4 2 − 4 2 2 | 43.96019 | 43.96022 | 1.8 | 39 |
| 3 2 1 − 2 2 1 | 20.31822 | 20.31823 | 1.4 | 78 | 4 1 4 − 2 1 2 | 43.97978 | 43.97978 | 0.4 | 38 |
| 4 0 4 − 3 2 2 | 20.46679 | 20.46676 | 1.8 | 56 | 4 0 4 − 2 0 2 | 44.37568 | 44.37566 | 0.5 | 33 |
| 3 1 2 − 2 1 2 | 21.60091 | 21.60090 | 1.6 | 98 | 5 3 2 − 4 1 4 | 44.81215 | 44.81214 | 1.0 | 40 |
| 4 1 4 − 3 1 2 | 22.37887 | 22.37890 | 1.7 | 79 | 6 1 5 − 5 1 5 | 45.14017 | 45.14023 | 1.2 | 20 |
| 5 2 3 − 4 4 1 | 22.99770 | 22.99783 | 1.7 | 20 | 6 2 5 − 5 0 5 | 45.47106 | 45.47117 | 1.6 | 21 |
| 3 2 2 − 2 0 2 | 23.90889 | 23.90890 | 1.3 | 67 | 5 4 1 − 4 2 3 | 45.64845 | 45.64846 | 1.1 | 40 |
| 2 2 0 − 0 0 0 | 23.91189 | 23.91190 | 0.9 | 31 | 4 2 3 − 2 2 1 | 45.75883 | 45.75879 | 0.8 | 35 |
| 4 2 3 − 3 2 1 | 25.44061 | 25.44060 | 1.7 | 99 | 6 3 4 − 5 1 4 | 46.30880 | 46.30870 | 1.7 | 23 |
| 5 0 5 − 4 2 3 | 25.64489 | 25.64487 | 1.1 | 44 | 4 1 3 − 2 1 1 | 46.95957 | 46.95957 | 1.0 | 38 |
| 4 3 2 − 3 3 0 | 26.40427 | 26.40426 | 1.6 | 74 | 4 2 2 − 2 2 0 | 47.25280 | 47.25283 | 0.6 | 29 |
| 4 3 1 − 3 3 1 | 26.64076 | 26.64078 | 1.9 | 69 | 5 5 1 − 4 3 1 | 48.75938 | 48.75924 | 1.3 | 21 |
| 5 1 5 − 4 1 3 | 26.86714 | 26.86713 | 1.4 | 50 | 5 5 0 − 4 3 2 | 48.96530 | 48.96522 | 1.5 | 26 |
| 3 3 1 − 2 1 1 | 27.25493 | 27.25497 | 0.9 | 43 | 6 4 3 − 5 2 3 | 49.82817 | 49.82820 | 1.4 | 17 |
| 4 2 2 − 3 2 2 | 27.73615 | 27.73613 | 1.2 | 92 | 5 0 5 − 3 2 1 | 51.08549 | 51.08552 | 1.2 | 17 |
| 3 3 0 − 2 1 2 | 28.65346 | 28.65354 | 0.8 | 57 | 5 4 2 − 4 0 4 | 51.22956 | 51.22941 | 1.7 | 15 |
| 4 1 3 − 3 1 3 | 29.42719 | 29.42710 | 1.4 | 98 | 4 2 2 − 2 0 2 | 51.64504 | 51.64509 | 1.7 | 29 |
| 5 1 4 − 3 3 0 | 52.64919 | 52.64938 | 1.6 | 14 | 5 3 3 − 3 1 3 | 69.17960 | 69.17960 | 1.3 | 30 |
| 6 4 2 − 5 2 4 | 53.12804 | 53.12801 | 1.3 | 15 | 5 4 1 − 3 2 1 | 71.08905 | 71.08900 | 1.2 | 28 |
| 4 3 1 − 2 1 1 | 53.89569 | 53.89558 | 1.8 | 31 | 6 2 5 − 4 2 3 | 71.11595 | 71.11601 | 0.9 | 28 |
| 6 5 2 − 5 3 2 | 54.91218 | 54.91233 | 0.9 | 14 | 5 4 2 − 3 2 2 | 71.69634 | 71.69629 | 1.3 | 27 |
| 4 3 2 − 2 1 2 | 55.05773 | 55.05776 | 1.6 | 26 | 6 1 5 − 4 1 3 | 72.00731 | 72.00740 | 1.1 | 25 |
| 6 5 1 − 5 3 3 | 55.63424 | 55.63413 | 1.5 | 11 | 6 3 4 − 4 3 2 | 72.55373 | 72.55369 | 1.7 | 22 |
| 5 1 5 − 3 1 3 | 56.29433 | 56.29427 | 1.4 | 38 | 6 4 3 − 4 4 1 | 72.82588 | 72.82579 | 0.9 | 11 |
| 5 0 5 − 3 0 3 | 56.49414 | 56.49406 | 1.4 | 39 | 6 4 2 − 4 4 0 | 73.03818 | 73.03812 | 1.4 | 9 |
| 4 4 0 − 2 2 0 | 58.13652 | 58.13653 | 0.9 | 25 | 6 3 3 − 4 3 1 | 74.06121 | 74.06125 | 1.6 | 20 |
| 4 4 1 − 2 2 1 | 58.27776 | 58.27784 | 0.8 | 25 | 6 2 4 − 4 224 | 74.34102 | 74.34102 | 1.8 | 23 |
| 5 2 4 − 3 2 2 | 58.53002 | 58.52995 | 1.4 | 43 | 5 5 0 − 3 3 0 | 75.36957 | 75.36951 | 1.7 | 18 |
| 5 3 3 − 3 3 1 | 59.45715 | 59.45717 | 1.8 | 25 | 5 5 1 − 3 3 1 | 75.40014 | 75.40025 | 0.9 | 14 |
| 5 1 4 − 3 1 2 | 59.70175 | 59.70170 | 1.8 | 44 | 5 4 1 − 3 0 3 | 76.49771 | 76.49782 | 1.6 | 12 |
| 5 3 2 − 3 3 0 | 60.13847 | 60.13839 | 1.7 | 26 | 6 3 3 − 4 1 3 | 80.99733 | 80.99737 | 1.5 | 22 |
| 5 2 3 − 3 2 1 | 60.95724 | 60.95735 | 1.3 | 38 | 6 2 4 − 4 0 4 | 81.61039 | 81.61035 | 1.9 | 19 |
| 6 1 5 − 4 3 1 | 65.07119 | 65.07117 | 2.2 | 10 | 6 3 4 − 4 1 4 | 83.63168 | 83.63165 | 2.2 | 24 |
| 5 2 3 − 3 0 3 | 66.36589 | 66.36596 | 1.5 | 33 | 6 4 2 − 4 2 2 | 83.92190 | 83.92191 | 1.5 | 19 |
| 5 3 2 − 3 1 2 | 67.19102 | 67.19098 | 0.8 | 31 | 6 4 3 − 4 2 3 | 85.34481 | 85.34474 | 2.0 | 20 |
| 6 1 6 − 4 1 4 | 68.53358 | 68.53357 | 1.1 | 32 | 6 5 1 − 4 3 1 | 88.45063 | 88.45057 | 0.8 | 14 |
| 6 0 6 − 4 0 4 | 68.61493 | 68.61501 | 0.8 | 21 | 6 5 2 − 4 3 2 | 88.64638 | 88.64661 | 2.2 | 14 |

[a] Mean experimental value of the individual GSCD and its rms deviation. [b] Here $n$ is the number of separate experimental GSCD obtained from the analysis of 74 absorption bands of the $CH_2D_2$ molecule recorded in the present study and used in the determination of the mean term value, and its $d_{rms}$.

## References and Notes


(1) Herzberg, G. *Molecular Spectra and Molecular Structure, Infrared and Raman Spectra of Polyatomic Molecules*, 1st ed.; van Nostrand: New York, 1945; *Vol. II*.

(2) Herzberg, G. *Molecular Spectra and Molecular Structure: Electronic Spectra and Electronic Structure of Polyatomic Molecules*; van Nostrand: Toronto, 1966; *Vol. III*.

(3) Wilson, E. B.; Decius, J. C.; Cross, P. C. *Molecular vibrations. The theory of infrared and Raman vibrational spectra*; McGraw-Hill: New York, 1955.

(4) Nielsen, H. H. *Phys. Rev.* **1941**, *60*, 794–810.

(5) Nielsen, H. H. *Phys. Rev.* **1945**, *68*, 181–191.

(6) Nielsen, H. H. *Rev. Mod. Phys.* **1951**, *23*, 90–136.

(7) Amat, G.; Nielsen, H. H.; Tarrago, G. *Rotation-vibration of polyatomic molecules: higher order energies and frequencies of spectral transitions*; Dekker: New York, 1971.

(8) Amat, G.; Goldsmith, M. *J. Chem. Phys.* **1955**, *23*, 1171–1172.

(9) Amat, G. *Cahiers Phys.* **1957**, *11*, 25.

(10) Mills, I. M. *A specialist periodical report/Royal Society of Chemistry. Theoretical chemistry.* **1974**; Vol. 1, p 110.

(11) Papousek, D.; Aliev, M. R. *Stud. Phys. Theor. Chem.* **1982**, *17*, 160.

(12) Califano, S. *Vibrational states*; Wiley: London etc., 1976.

(13) Chen, C. L.; Maessen, B.; Wolfsberg, M. *J. Chem. Phys.* **1985**, *83*, 1795–1807.

(14) Maessen, B.; Wolfsberg, M.; Harding, L. B. *J. Phys. Chem.* **1985**, *89*, 3324–3325.

(15) Maessen, B.; Wolfsberg, M. *J. Phys. Chem.* **1985**, *89*, 3876–3879.

(16) Maessen, B.; Wolfsberg, M. *J. Chem. Phys.* **1984**, *80*, 4651–4662.

(17) Partridge, H.; Schwenke, D. W. *J. Chem. Phys.* **1997**, *106*, 4618–4639.

(18) Schwenke, D. W.; Partridge, H. *J. Chem. Phys.* **2000**, *113*, 6592–6597.

(19) Shirin, S. V.; Polyansky, O. L.; Zobov, N. F.; Ovsyannikov, R. I.; Csaszar, A. G.; Tennyson, J. *J. Mol. Spectrosc.* **2006**, *236*, 216–223.

(20) Maksyutenko, P.; Rizzo, T. R.; Boyarkin, O. V. *J. Chem. Phys.* **2006**, *125*, 181101.

(21) Tennyson, J.; Kostin, M. A.; Barletta, P.; Harris, G. J.; Polyansky, O. L.; Ramanlal, J.; Zobov, N. F. *Comput. Phys. Commun.* **2004**, *163*, 85–116.

(22) Luckhaus, D. *J. Chem. Phys.* **2000**, *113*, 1329–1347.

(23) Quack, M.; Suhm, M. A. *J. Chem. Phys.* **1991**, *95*, 28–59.

(24) Klopper, W.; Quack, M.; Suhm, M. A. *Chem. Phys. Lett.* **1996**, *261*, 35–44.

(25) Klopper, W.; Quack, M.; Suhm, M. A. *J. Chem. Phys.* **1998**, *108*, 10096–10115.

(26) Zhang, D. H.; Wu, Q.; Zhang, J. Z. H.; von Dirke, M.; Bacic, Z. *J. Chem. Phys.* **1995**, *102*, 2315–2325.

(27) Kuhn, B.; Rizzo, T. R.; Luckhaus, D.; Quack, M.; Suhm, M. A *J. Chem. Phys.* **1999**, *111*, 2565–2587; 135 pages of supplementary material published as AIP Document No PAPS JCPS A6-111-302905 by American Institute of Physics, Physics Auxiliary Publication Service, 500 Sunnyside Blvd., Woodbury, N. Y. 1179-29999.

(28) Fehrensen, B.; Luckhaus, D.; Quack, M. *Chem. Phys. Lett.* **1999**, *300*, 312–320.

(29) Fehrensen, B.; Luckhaus, D.; Quack, M. *Chem. Phys.* **2007**, *338*, 90–105.

(30) Peyerimhoff, S. D.; Lewerenz, M.; Quack, M. *Chem. Phys. Lett.* **1984**, *109*, 563–569.

(31) Lewerenz, M.; Quack, M. *J. Chem. Phys.* **1988**, *88*, 5408–5432.

(32) Carrington, T.; Halonen, L.; Quack, M. *Chem. Phys. Lett.* **1987**, *140*, 512–519.

(33) Halonen, L.; Carrington, T.; Quack, M. *J. Chem. Soc., Faraday Trans. 2* **1988**, *84*, 1371–1388.

(34) Marquardt, R.; Quack, M. *J. Chem. Phys.* **1991**, *95*, 4854–4876.

(35) Marquardt, R.; Quack, M. *J. Chem. Phys.* **1998**, *109*, 10628–10643.

(36) Marquardt, R.; Quack, M. *J. Phys. Chem. A* **2004**, *108*, 3166–3181.

(37) Schwenke, D. W.; Partridge, H. *Spectrochim. Acta, Part A* **2001**, *57*, 887–895.

(38) Schwenke, D. W. *Spectrochim. Acta, Part A* **2002**, *58*, 849–861.

(39) Hollenstein, H.; Marquardt, R. R.; Quack, M.; Suhm, M. A. *J. Chem. Phys.* **1994**, *101*, 3588–3602.

(40) Wang, X. G.; Carrington, T. *J. Chem. Phys.* **2003**, *118*, 6260–6263.

(41) Wang, X. G.; Carrington, T. *J. Chem. Phys.* **2003**, *119*, 94–100.

(42) Wang, X. G.; Carrington, T. *J. Chem. Phys.* **2003**, *119*, 101–117.

(43) Yu, H. G. *J. Chem. Phys.* **2004**, *121*, 6334–6340.

(44) Oyanagi, C.; Yagi, K.; Taketsugu, T.; Hirao, K. *J. Chem. Phys.* **2006**, *124*, 064311.

(45) Marquardt, R.; Quack, M.; Thanopulos, I. *J. Phys. Chem. A* **2000**, *104*, 6129–6149.

(46) Ulenikov, O. N.; Bekhtereva, E. S.; Grebneva, S. V.; Hollenstein, H.; Quack, M. *Phys. Chem. Chem. Phys.* **2005**, *7*, 1142–1150.

(47) Ulenikov, O. N.; Bekhtereva, E. S.; Grebneva, S. V.; Hollenstein, H.; Quack, M. *Mol. Phys.* **2006**, *104*, 3371–3386.

(48) Wilmshurst, J. K.; Bernstein, H. J *Can. J. Chem.-Rev. Can. Chim.* **1957**, *35*, 226–235.

(49) Olson, W. B.; Plyler, E. K.; Allen, H. C. *J. Res. Natl. Bur. Stand. Sect. A-Phys. Chem.* **1963**, *67*, 27.

(50) Morillon-Chapey, M.; Alamichel, C. *Can. J. Phys* **1973**, *51*, 2189–2196.

(51) Deroche, J. C.; Guelachvili, G. *J. Mol. Spectrosc.* **1975**, *56*, 76–87.

(52) Deroche, J. C.; Graner, G.; Cabana, A. *J. Mol. Spectrosc.* **1975**, *57*, 331–347.

(53) Deroche, J. C.; Pinson, P. *J. Mol. Spectrosc.* **1975**, *58*, 229–238.

(54) Deroche, J. C.; Graner, G.; Bendtsen, J.; Brodersen, S. *J. Mol. Spectrosc.* **1976**, *62*, 68–79.

(55) Akiyama, M.; Nakagawa, T.; Kuchitsu, K. *J. Mol. Spectrosc.* **1977**, *64*, 109–124.

(56) Ulenikov, O. N.; Malikova, A. B.; Shevchenko, G. A.; Guelachvili, G.; Morillon-Chapey, M. *J. Mol. Spectrosc.* **1991**, *149*, 160–166.

(57) Ulenikov, O. N.; Malikova, A. B.; Shevchenko, G. A.; Guelachvili, G.; Morillon-Chapey, M. *J. Mol. Spectrosc.* **1992**, *154*, 22–29.

(58) Ulenikov, O. N.; Malikova, A. B.; Guelachvili, G.; Morillon-Chapey, M. *J. Mol. Spectrosc.* **1993**, *159*, 422–436.

(59) Ulenikov, O. N.; Tolchenov, R. N.; Koivusaari, M.; Alanko, S.; Anttila, R. *J. Mol. Spectrosc.* **1994**, *167*, 109–130.

(60) Ulenikov, O. N.; Hirota, E.; Akiyama, M.; Alanko, S.; Koivusaari, M.; Anttila, R.; Guelachvili, G.; Tolchenov, R. N. *J. Mol. Spectrosc.* **1996**, *180*, 423–432.

(61) Hollenstein, H.; Marquardt, R.; Quack, M.; Suhm, M. A. *Ber. Bunsenges. Phys. Chem.* **1995**, *99*, 275–281.

(62) Signorell, R.; Marquardt, R.; Quack, M.; Suhm, M. A. *Mol. Phys.* **1996**, *89*, 297–313.

(63) Albert, S.; Bauerecker, S.; Boudon, V.; Brown, J. M.; Champion, J. P.; Loete, M.; Nikitin, A.; Quack, M. *Chem. Phys.* **2009**, *356*, 131−148.

(64) Niederer, H. M.; Albert, S.; Bauerecker, S.; Boudon, V.; Champion, J. P.; Quack, M. *Chimia* **2008**, *62*, 273–276.

(65) Hippler, M.; Quack, M. *J. Chem. Phys.* **2002**, *116*, 6045–6055.

(66) Quack, M. *Chimia* **2003**, *57*, 147–160.

(67) Albert, S.; Albert, K. K.; Quack, M. *Trends in Optics and Photonics (TOPS)*; Optical Society of America: Washington DC, 2003; *Vol. 84*, pp 177−180.

(68) Albert, S.; Quack, M. *ChemPhysChem* **2007**, *8*, 1271–1281.

(69) Albert, S.; Bauerecker, S.; Quack, M.; Steinlin, A. *Mol. Phys.* **2007**, *105*, 541–558.

(70) Bauerecker, S.; Taraschewski, M.; Weitkamp, C.; Cammenga, H. K. *Rev. Sci. Instrum.* **2001**, *72*, 3946–3955.

(71) Bauerecker, S.; Taucher, F.; Weitkamp, C.; Michaelis, W.; Cammenga, H. K. *J. Mol. Struct.* **1995**, *348*, 237–241.

(72) Bauerecker, S. *Phys. Rev. Lett.* **2005**, *94*, 033404.

(73) Ulenikov, O. N.; Bekhtereva, E. S.; Bauerecker, S.; Albert, S.; Hollenstein, H.; Quack, M. High Resolution Spectroscopy and Dynamics of the Methane Molecule: $CH_2$ $D_2$ Isotopomer. In *Proceedings Nineteenth Colloquium on High Resolution Molecular Spectroscopy, Salamanca, Spain, 11−16 September 2005*, Paper N10, p. 395; Bermejo, D., Doménech, J. L., Moreno, M. A., Eds.; Sociedad Española de Óptica: Salamanca, 2005; ISBN 84-609-6737-9.

(74) Maki, A. G.; Wells, J. S. *Wavenumber Calibration Tables from Heterodyne Frequency Measurements*, Volume 821 of NIST Spec. Publ. ; National Institute of Standards and Technology: Washington, 1991.

(75) Rothman, L. S.; et al. *J. Quant. Spectrosc. Radiat. Transfer* **2005**, *96*, 139–204.

(76) Bekhtereva, E. S.; Ulenikov, O. N.; Albert, S.; Bauerecker, S.; Hollenstein, H.; Quack, M. *Proceedings of the 20th Colloquium on High-Resolution Molecular Spectroscopy*, Paper L7, pp 288−289; Boudon, V., Ed.; Université de Dijon: Dijon, 2007, and in preparation..

(77) Longuet-Higgins, H. C. *Mol. Phys.* **1963**, *6*, 445–460.

(78) Quack, M. *Mol. Phys.* **1977**, *34*, 477–504.

(79) Pepper, M. J. M.; Shavitt, I.; v. Ragué Schleyer, P.; Glukhovtsev, M. N.; Janoschek, R.; Quack, M. *J. Comput. Chem.* **1995**, *16*, 207–225.

(80) Bekhtereva, E. S.; Ulenikov, O. N.; Sinitsin, E. A.; Albert, S.; Bauerecker, S.; Hollenstein, H.; Quack, M. On the semi-empirical determination of the methane potential energy surface. In *Proceedings of the 20th Colloquium on High-Resolution Molecular Spectroscopy*, Paper J30, p 268; Boudon, V., Ed.; Université de Dijon: Dijon, 2007 and in preparation.

(81) Watson, J. K. G. *Mol. Phys.* **1968**, *15*, 479–490.

(82) Luckhaus, D.; Quack, M. *Mol. Phys.* **1989**, *68*, 745–758.

(83) Lee, T. J.; Martin, J. M. L.; Taylor, P. R. *J. Chem. Phys.* **1995**, *102*, 254–261.

(84) Raynes, W. T.; Lazzeretti, P.; Zanasi, R.; Sadlej, A. J.; Fowler, P. W. *Mol. Phys.* **1987**, *60*, 509–525.

(85) Gray, D. L.; Robiette, A. G. *Mol. Phys.* **1979**, *37*, 1901–1920.

(86) Duncan, J. L.; Law, M. M. *Spectrochim. Acta, Part. A* **1997**, *53*, 1445–1457.

(87) Blunt, V. M.; Mina-Camilde, N.; Cedeno, D. L.; Manzanares, C. *Chem. Phys.* **1996**, *209*, 79–90.

(88) Quack, M. *J. Chem. Phys.* **1985**, *82*, 3277–3283.

(89) Ulenikov, O. N.; Bekhtereva, E. S.; Albert, S.; Bauerecker, S.; Hollenstein, H.; Quack, M., in preparation.

(90) Ulenikov, O. N.; Bekhtereva, E. S.; Sinitsin, E. A.; Albert, S.; Hollenstein, H.; Quack, M. On the Global Analysis of the $CH_3D$ Rovibrational Energies. In *Book of Abstracts of the 20th International Conference on High Resolution Molecular Spectroscopy, Praha 2008*, Paper D27, p 71; Bludský, O., Pracna, P., Urban, Š., Eds.; ICT Press: Praha, 2008, ISBN 978-80-7080-689-0.

JP809839T